BACHELOR THESIS

Advanced Technology

CONTACT MECHANICS IN MSC ADAMS

A technical evaluation of the contact models in multibody dynamics software MSC Adams

Author

Jochem Giesbers

Faculty of Engineering Technology

Applied Mechanics

Examination Committee

Chairperson:	Prof. Dr. Ir. A. de Boer
Supervisor:	Dr. Ir. M.H.M. Ellenbroek
External examiner:	Dr. H.K. Hemmes
Member:	Dr. Ir. P.J.M. van der Hoogt

UNIVERSITY OF TWENTE.

July 11th, 2012

Abstract:

The goal of this study is to gain insight in the modelling of (physical) contact in Adams, a product by MSC Software. Adams is the most widely used multibody dynamics and motion analysis software in the world. The aim is to establish an understanding of contact in Adams and the relation to the laws of physics. First, the algorithms and formulas used by Adams are analysed. Second, a variety of models is simulated and the effects of the corresponding variables are analysed. After this study the acquired knowledge can be used to model more complex systems in Adams.

Table of Contents

1. Introduction:

This report has been written to finalize the bachelor Advanced Technology assignment that has been done in the Applied Mechanics research chair of the University of Twente.

Contact between objects is an important aspect in multibody dynamics. It is a discontinuous, non-linear phenomenon and therefore requires iterative calculations. Adams, a MSC Software product in multibody dynamics, performs these calculations and can provide accurate results. The accuracy depends on user-defined values, so it is of importance that the user has knowledge of the program, the algorithms and the variables.

This report shall first deal with the relevant theory and background information of contact forces and three built-in contact methods of Adams; the IMPACT function model, the POISSON restitution model and the Coulomb friction model. Subsequently these three contact methods are evaluated and discussed by the use of two self-constructed Adams models. All parameters in these three contact methods are varied to research their effect on the contact behaviour. Subsequently the recommended values for all the parameters are determined. Finally, conclusions are drawn and recommendations for further research are made.

A word of thanks extends to my supervisor Dr. Ir. M.H.M. Ellenbroek for providing insight, help and understanding throughout the process of this bachelor assignment.

2. *Theory:*

2.1 Hertzian contact theory

In contact mechanics there are multiple models for predicting contact forces and geometrical deformations. In 1882, Heinrich Hertz published a theory concerning circular contact areas and elastic deformations in the case of contact between two spheres[1]. In this theory the Van der Waals interactions and other adhesive interactions are neglected. It was not until 1970 that Johnson, Kendall and Roberts published a theory that is largely the same, but includes adhesion in the contact area[2].

Hertzian theory is based on a set of assumptions, which are as follows:

- Adhesion is neglected. Contacting bodies can be separated without adhesion forces.
- Surfaces are continuous and non-conforming, i.e. the initial contact is a point or a line.
- Pressures within the materials are small enough to cause only elastic deformations.
- The area of contact is much smaller than the characteristic radius of the body.
- The surfaces are perfectly smooth, i.e. only a normal force acts between the parts in contact.

Consider two objects brought into physical contact through the action of applied forces. The contact area depends on the geometry of the contacting bodies, the load, and the material properties. The contact area between two parallel cylinders is a narrow rectangle. Two, non-parallel cylinders have an elliptical contact area, unless the cylinders are crossed at 90 degrees, in which case they have a circular contact area. Two spheres also have a circular contact area, which is merely a special case of elliptical contact. The associated pressure distribution is semi-ellipsoidal.

Figure 1[3] shows a side view of two objects (turquoise and orange) in contact. The grey area represents a top view of the elliptical contact area, with the yellow areas being the semi-ellipsoidal pressure distributions in both dimensions.

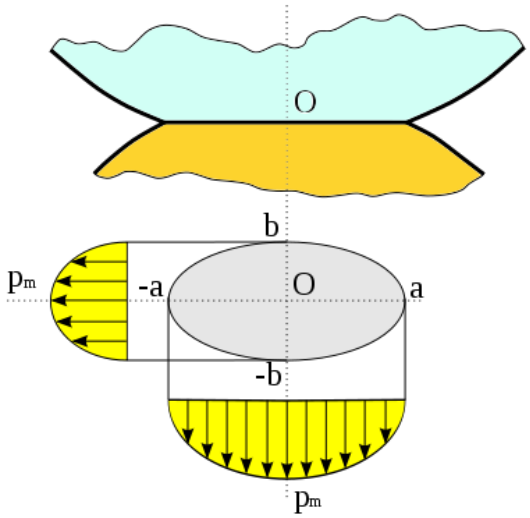

Figure 1: Schematic representation of Hertzian contact

The contact stiffness depends on the material properties of both objects, through the following equations[4]:

Contact stiffness: $k_c = 2aE^*$

Hertz contact radius: $a = \left(\frac{3LR}{4E^*}\right)^{1/3}$

Combined Young's Modulus: $E^* = \left(\frac{1-\nu_1^2}{E_1} + \frac{1-\nu_2^2}{E_2}\right)^{-1}$

Combined radius of curvature: $R = \left(\frac{1}{R_1} + \frac{1}{R_2}\right)^{-1}$

Applied normal force (load): L

[1] H. Hertz, Über die berührung fester elastischer Körper (On the contact of rigid elastic solids). In: Miscellaneous Papers. Jones and Schott, Editors, J. reine und angewandte Mathematik 92, Macmillan, London (1896), p. 146 English translation: Hertz, H.

[2] K. L. Johnson and K. Kendall and A. D. Roberts, Surface energy and the contact of elastic solids, Proc. R. Soc. London A 324 (1971) 301-313

[3] Contact Mechanics, Wikipedia; http://en.wikipedia.org/wiki/File:Hertz.svg

[4] University of Washington, course: Molecular Properties of Gases, Liquids and Solids (ChemE498), handout 'Contact Mechanics', p2-5

2.2 Hertzian contact theory in relation to the IMPACT function

This chapter is based on a misconception and therefore contains incorrect information.

One of the methods that Adams uses is extrapolated from Hertzian contact theory: the Adams IMPACT function. A detailed description of the IMPACT function will follow in Chapter 2.6. A brief description of the relation between the IMPACT function and the Hertzian contact theory as described in Chapter 2.1 will follow now.

In Chapter 2.1 a set of formulas for the contact stiffness was proposed, from which the normal force follows:

$$F = k_c(x_1 - x) = 2aE^*(x_1 - x) = 2\left(\frac{3L\left(\frac{1}{R_1}+\frac{1}{R_2}\right)^{-1}}{4\left(\frac{1-v_1^2}{E_1}+\frac{1-v_2^2}{E_2}\right)^{-1}}\right)^{1/3}\left(\frac{1-v_1^2}{E_1}+\frac{1-v_2^2}{E_2}\right)^{-1}(x_1 - x)$$

In the formula above a linear spring force can be recognized (if k_c would be constant). Its value depends on a stiffness parameter k_c and the penetration depth $(x_1 - x)$. The stiffness depends on both materials' Young's Moduli and Poisson's Ratios, both objects' radii and the force with which the objects are pressed together. The IMPACT function uses a stiffness parameter that is related to the Hertzian contact stiffness. However, the load L appears to vary with the penetration depth. A greater penetration depth leads to a greater restoring normal force (L). Therefore the contact stiffness is not constant, making the force non-linear. It is believed that because of this non-linearity, the IMPACT function does not only use a static stiffness parameter (k), but also an additional force exponent (e):

$$F = k(x_1 - x)^e$$

In this formula the stiffness k is constant, so the non-linearity encountered in the previous paragraph will have to be modeled with the force exponent e. This way the effective contact stiffness is not constant and follows the Hertzian contact theory closer than a constant stiffness would do. It should be noted that the value of the force exponent e should be greater than 1, to increase the contact stiffness for increasing penetration depths. Chapter 2.6 and Figure 5 show this in graphic detail.

Hertzian contact theory states that at contact, both objects deform ever so slightly to create an elliptical contact area. Deformation dissipates energy from the system, so the IMPACT function has to take this dissipation into account. Adams uses a damping parameter to create a damping force that dissipates energy from the system. Since the dissipation of energy depends on the contact area and contact stiffness, the damping value in the IMPACT function is recommended to be a small fraction of the stiffness value, according to some sources: $c_{max} < 0.01k$.

Chapter 2.6 will further explore the IMPACT function and all of its parameters.

2.3 Geometry engines

Contact forces consist of two components, which both have a separate physical meaning. One component is in the direction of the common normal (of the surface of contact) and the other component is perpendicular to this normal. The first is called the normal force and the latter is called the tangential force, or more commonly known as friction. In order for Adams to calculate these components, it is necessary to determine the contact point(s) and the common normal of the contact. Adams uses one of the two built-in geometry engines to determine these. The two engines are Parasolid and RAPID, the latter being the default engine.

Parasolid[5] is the world's leading 3D solid modeling component software used as the foundation of Siemens PLM's NX and Solid Edge products. Parasolid is also licensed to many of the leading independent software vendors, one of which is MSC Software. Adams can use Parasolid – if it is selected instead of RAPID – to determine geometrical aspects of the 3D contacts that occur during simulations. It is an exact boundary-representation geometric modeler, which means that objects have exact surfaces. Curved surfaces are truly curved and do not consist of polygons. Because surfaces are not divided in smaller parts, their representation is as accurate as possible. The simulation times are relatively high when using Parasolid.

RAPID[6] is the abbreviation of Rapid and Accurate Polygon Interference Detection. It is a software package developed by the Department of Computer Science at the University of North Carolina. When RAPID is selected in Adams, which is the default geometry engine, objects are divided in a large amount of polygons. RAPID's algorithm pre-computes a hierarchical representation of the Adams model using tight-fitting oriented bounding box trees (OBBTrees)[7]. Figure 2 shows how this hierarchy is created. During simulations, the algorithm traverses two such trees and tests for overlaps between oriented bounding boxes. This method is less accurate than the exact boundary-representation of Parasolid, because of the use of polygons. The advantage of RAPID is that it is faster than Parasolid.

The user has the capability of switching between the engines. For this bachelor assignment the default engine, RAPID, is used.

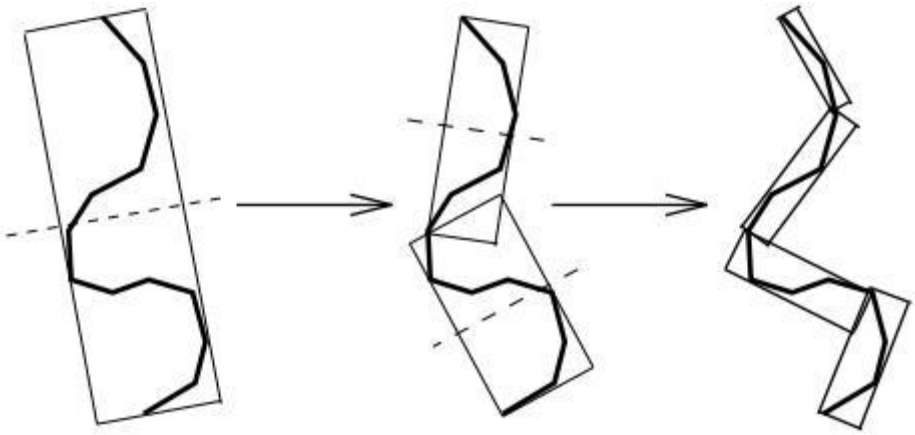

Figure 2: Building the OBBTree: recursively partition of polygons

[5] Siemens PLM Software, http://www.plm.automation.siemens.com/nl_nl/products/open/parasolid/index.shtml

[6] GAMMA research group, University of North Carolina, http://gamma.cs.unc.edu/OBB/

[7] S. Gottschalk, M.C. Lin, D. Manocha, OBBTree: A Hierarchical Structure for Rapid Interference Detection, http://www.stanford.edu/class/cs340v/papers/obbtree.pdf

2.4 Normal force

The normal force is the contact force's component in the direction of the common normal, which may coincide with the total contact force, given that there is no friction. A common situation is an object resting on a surface. In this case the value of the normal force depends on only the object's mass and the gravitational acceleration:

$$F_n = mg$$

If the surface were to be on an angle, the value of the normal force would depend on this angle, too:

$$F_n = mg\cos\theta$$

In this particular situation, the direction of the normal force is trivial. In more complex situations (e.g. three-dimensional), the direction of this common normal can be determined by Adams' geometry engine. Another complexity is when the object is not stationary, but is subjected to a force/acceleration other than just gravity. In case of a collision, the flexibility of the objects plays a part. If both objects were to have infinite stiffness, the acceleration would approach infinity. It is exactly this aspect of the normal force that is discontinuous and thus non-linear. In Chapter 2.6 and 2.7 it will be discussed how Adams models this flexibility, in order to create a finite normal force.

2.5 Friction

There are several types of friction. The tangential component of the contact force is called dry friction. An approximate model used to calculate this force is called Coulomb friction. This force can be divided into two regimes, static friction and kinetic friction. The first occurs when two objects have a relative velocity of exactly zero. The latter occurs when this relative velocity is non-zero. Both static and kinetic friction are related to the normal force discussed earlier, by respectively the coefficient of static friction (μ_s) and the coefficient of kinetic friction $(\mu_k$ or $\mu_d)$, which are both dimensionless scalars:

$$F_s \leq \mu_s F_n \text{ (static friction)}$$
$$F_d = \mu_d F_n \text{ (kinetic friction)}$$

The values of the coefficients are empirical measurements and are usually between 0 and 1, but have been seen to go up to 1.5 or even higher.

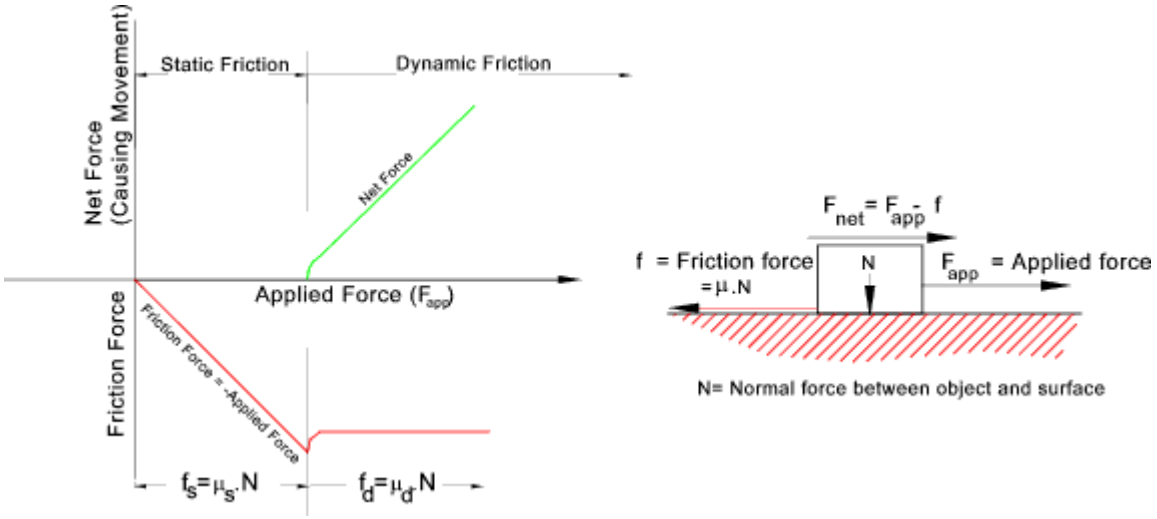

Figure 3: Visualisation of Coulomb friction

Figure 3 shows that static friction opposes any applied force, as long as the object does not move and remains in the static regime. Once the velocity becomes non-zero, the static friction $F_s = \mu_s F_n$ makes a transition to kinetic friction $F_d = \mu_d F_n$, which is constant for every non-zero velocity. The transitional phase appears in the figure as a discontinuity.

In Chapter 2.8 it will be discussed how Adams models the frictional force.

2.6 Contact feature: IMPACT function model

Figure 4 shows the dialog box 'Create Contact' in MSC Adams. If a user of Adams creates a contact between two bodies, a model must be chosen for the calculation of the normal force. A choice is given between the IMPACT function model and the POISSON model (Restitution). It is also possible to define a custom function, but this goes beyond the scope of this study.

After choosing the IMPACT function model, four variables must be defined; stiffness, force exponent, damping and penetration depth. These correspond to four arguments in the actual IMPACT function, which will be discussed now.

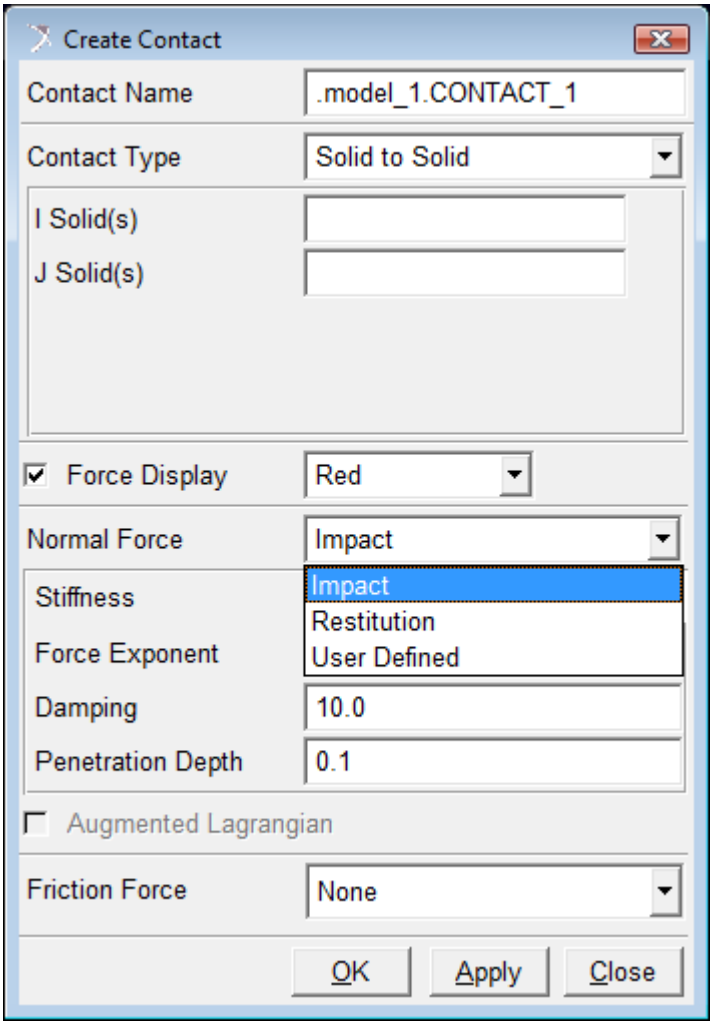

Figure 4 (right): Dialog box 'Create Contact'; IMPACT chosen as model

The IMPACT function has seven arguments, which all correspond to properties of the physical world:

$$IMPACT(x, \dot{x}, x_1, k, e, c_{max}, d)$$

x	An expression that specifies a distance variable used to compute the IMPACT function.
$\dot{x}$	An expression that specifies the time derivative of x to IMPACT.
x_1	A positive real variable that specifies the free length of x. If x is less than x_1, then Adams calculates a positive value for the force. Otherwise, the force value is zero.
k	A non-negative real variable that specifies the stiffness of the boundary surface interaction.
e	A positive real variable that specifies the exponent of the force deformation characteristic. For a stiffening spring characteristic, e > 1.0. For a softening spring characteristic, 0 < e < 1.0.
c_{max}	A non-negative real variable that specifies the maximum damping coefficient.
d	A positive real variable that specifies the boundary penetration at which Adams applies full damping.

The first three arguments are determined every time step of the simulation and are geometry-related expressions. The other four arguments are the user-specified parameters seen in the dialog box in Figure 4.

$$F = \begin{cases} 0 & \text{if } x > x_1 \\ k(x_1 - x)^e - c_{max}\dot{x} * STEP(x, x_1 - d, 1, x_1, 0) & \text{if } x \leq x_1 \end{cases}$$

The IMPACT function[8] is written out above. It can be seen that it activates when the distance between the two objects is smaller than the free length of x. When so, the force becomes non-zero and consists of two parts: an exponential spring force and a damping force that follows a step function. It should be noted that both forces are strictly positive. The reason is that the calculated normal force should oppose the compression that occurs during penetration. Negative forces would support the compression, which a real normal force would never do.

As soon as x becomes smaller than x_1, a positive spring force is created, assuming that k is positive as it is supposed to be. Unlike in a linear spring ($F = -kx$), the spring force is exponential. For $0 < e < 1$, the spring force concaves down and at $x = 0$, the slope is infinite. For $e = 1$, the spring force is linear, so at $x = 0$, the slope has a finite value. For $e > 1$, the spring force concaves up and at $x = 0$, the slope is zero. It is recommended to use $e > 1$, so that the slope of the spring force is continuous even when passing from the non-contact domain to the contact domain. From experience it can be said that hard metals require a value of $e \approx 2.2$, softer metals require a value of $e \approx 1.5$ and softer materials like rubber require a value of $e \approx 1.1$. From Hertzian contact theory follows that the stiffness of the contact, k, is based on both material properties (Young's Modulus and Poisson's Ratio)and geometrical properties (radius of curvature). Determining the value can be done by trial-and-error or by consulting experience of other users.

Since the relative velocity will have a non-zero value when x becomes smaller than x_1, a linear damper ($F = -c\dot{x}$) would induce a discontinuity in the damping force. To avoid this problem, a cubic step function is used to increase the damping force from zero to $c_{max}\dot{x}$ within the penetration depth d. It should be noted that the penetration depth d is not necessarily the maximum penetration depth during a collision. It is merely a penetration depth at which the damping is at maximum.

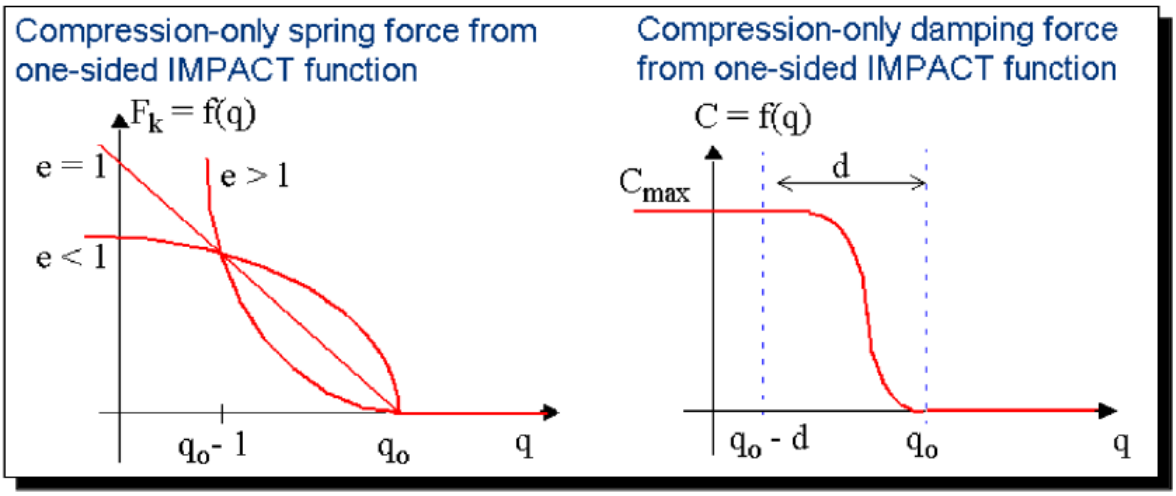

Figure 5: Graphs of the two force components of the IMPACT function

Figure 5[9] shows the behaviour of the IMPACT function's spring force and damping force. Recommended values are: $e > 1$; $d = 0.01\ mm$; $c_{max} < 0.01k$.

The IMPACT function will be used in several cases, later in this report. In these cases the effect of the variables on the dynamic behaviour will be shown.

[8] MSC Software, Adams/Solver help, p33; http://simcompanion.mscsoftware.com/infocenter/index?page=content&id=DOC9391

[9] Chris Verheul, 'Contact Modeling' presentation, sheet 9; http://www.insumma.nl/wp-content/uploads/SayField_Verheul_ADAMS_Contacts.pdf

2.7 Contact feature: POISSON restitution model

The second built-in method for calculating the normal forces is called Restitution in Adams. Most important in this method is the so-called restitution coefficient. From now on it will be called COR, Coefficient Of Restitution. It defines a continuum between a perfectly elastic (COR = 1.0) and perfectly inelastic (COR = 0.0) collision.

The difference between both limits is that in an elastic collision the kinetic energy is conserved and in an inelastic collision the kinetic energy is not conserved. In a perfectly inelastic collision the reduction of kinetic energy equals the total kinetic energy before the collision in a center-of-momentum frame. Even though the behaviour of kinetic energy differs in these cases, in all collisions the total momentum is conserved.

For simple collisions the object velocities can be calculated with the conservation of momentum and the definition of COR:

$$COR = \frac{v_b - v_a}{u_a - u_b}$$
$$m_a u_a + m_b u_b = m_a v_a + m_b v_b$$

From these equations the velocities v_a and v_b can be derived:

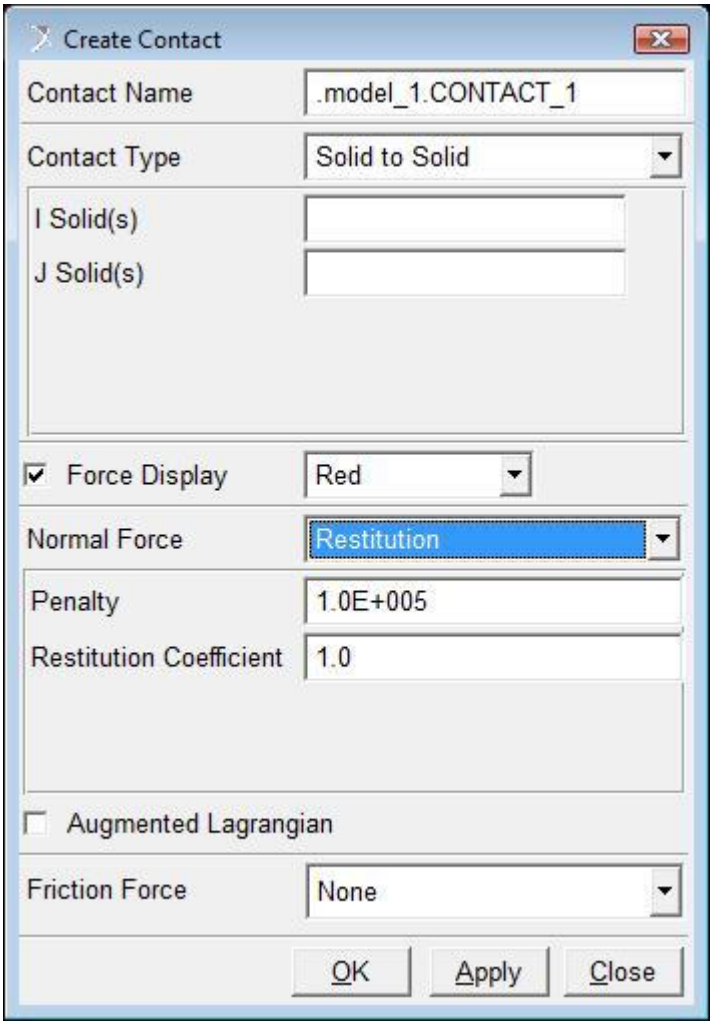

Figure 6: Dialog box 'Create Contact'; Restitution chosen as model

$$v_a = \frac{m_a u_a + m_b u_b + m_b COR(u_b - u_a)}{m_a + m_b} \qquad v_b = \frac{m_a u_a + m_b u_b + m_a COR(u_a - u_b)}{m_a + m_b}$$

Adams calculates the normal force, not the velocity. This is done with use of a penalty parameter, which is similar to a stiffness parameter. The disadvantage of using this so-called penalty regularization is that the user is responsible for setting an appropriate penalty parameter. A small value will result in disobeying the impenetrability constraint (no negative gap between objects) and therefore inaccurate results. If the penalty parameter approaches infinity, the impenetrability constraint would be perfectly met. Integration difficulties will arise, though. In a MMKS (mm,kg,N,s,deg) unit model, a value of 1E5 or 1E6 is appropriate.

The function for the normal force associated with the POISSON restitution model is:

$$F = p(\varepsilon - 1)\dot{x}$$

In which p is the penalty parameter, ε is COR and $\dot{x}$ is the time derivative of x, the gap. The relation of this formula to the theory described above is $\dot{x} = v_a - v_b$, with the order of a and b depending on the object order.

2.8 Contact feature: Coulomb friction

Whereas the normal force is mandatory, (Coulomb) friction is optional in the Adams contact feature.

In Chapter 2.5 it was discussed that frictional force (and coefficient of friction μ) instantly jumps from zero to a finite, non-zero value when the relative velocity between the objects becomes non-zero. Adams, however, does model this discontinuity as a continuity, displayed in Figure 8. When the value of the stiction transition velocity (V_s) approaches zero, the closer the model approaches stiction. However, Adams does not allow $V_s = 0$, so it is impossible to model perfect stiction.

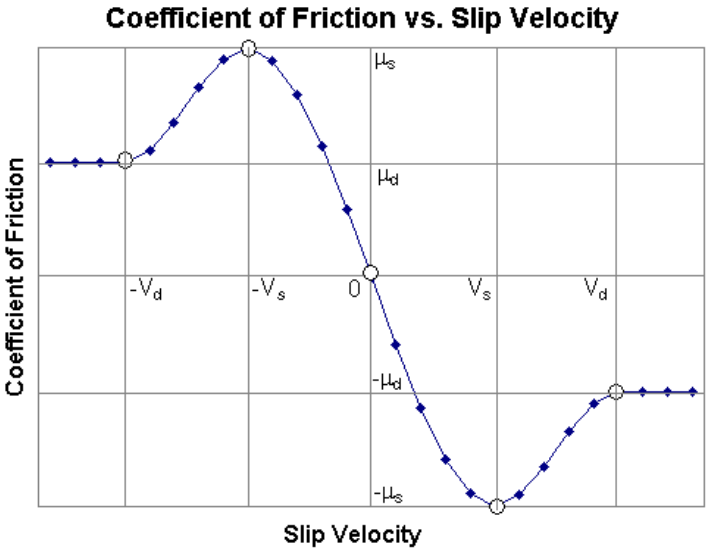

Figure 7 (top-right): Representation of the coefficient of friction function

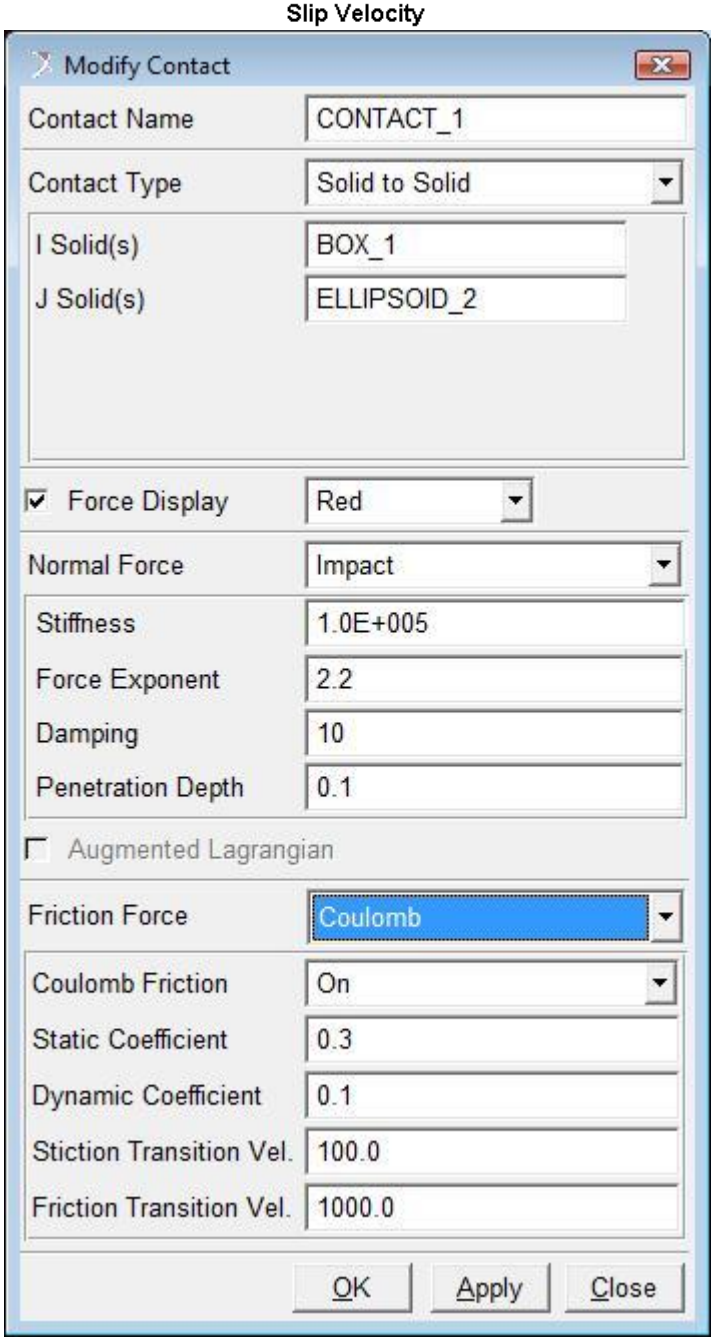

Figure 8 (bottom-right): Dialog box 'Create Contact'; Coulomb friction activated

The function follows cubic step functions from respectively $-\mu_d$ to $-\mu_s$, $-\mu_s$ to $+\mu_s$ and $+\mu_s$ to $+\mu_d$. In other intervals ($|v| \geq V_d$) the coefficient of friction is equal to $\pm\mu_d$.

The four characteristics (μ_s, μ_d, V_s, V_d) are user-specified in the dialog window. As said before, the static and dynamic coefficients are often between 0 and 1. In Chapter 4, values for these coefficients can be found for different contact materials. These values are empirical. The dynamic coefficient is typically lower than the static coefficient, reflecting the common experience that it is easier to keep something in motion across a horizontal surface than to start it in motion from rest. It is important to know that the friction transition velocity (V_d) is greater than the stiction transition velocity (V_s) by definition.

With the four user-specified values, Adams can calculate coefficients of friction for every slip velocity. This coefficient must be multiplied by the normal force to determine the actual friction force. So the choices made in the calculation of the normal force are important for the calculation of the friction force, too.

3. Cases:

3.1 Introduction

In this chapter a set of two models will be discussed. The first model considers a sphere bouncing on a fixed box element that resembles the ground. With this model, the effect of all variables in both the IMPACT function model and POISSON restitution model will be illustrated. The second model considers a sphere rolling on top of a fixed box element. With this model, the effect of all variables in the Coulomb friction model will be illustrated. Each case starts with a model description including a screenshot from Adams. The two cases contain lists of observed effects when varying one variable. For each variable a list is included. Both of these cases end with a discussion including explanations for observed phenomena.

At the end of this chapter we will have established an insight in the effects of all the variables associated with the Adams contact feature.

Plotted graphs that are referred to in the cases can be found in Appendices A and B.

3.2 Bouncing ball (2D)

In the first case the behaviour of a sphere, with an infinite stiffness, falling onto a plane is observed. Since the movement is purely vertical, friction plays no role and is turned off. To illustrate what the different variables of the IMPACT function model and POISSON restitution model do, the Y-coordinate of the sphere's center-of-mass is analysed, which is initially 0.4 meters and collides with the floor at 0.0 meters.

First the IMPACT function model is researched and second the POISSON restitution model. The findings of this research on both models will then be discussed in the last part of this case.

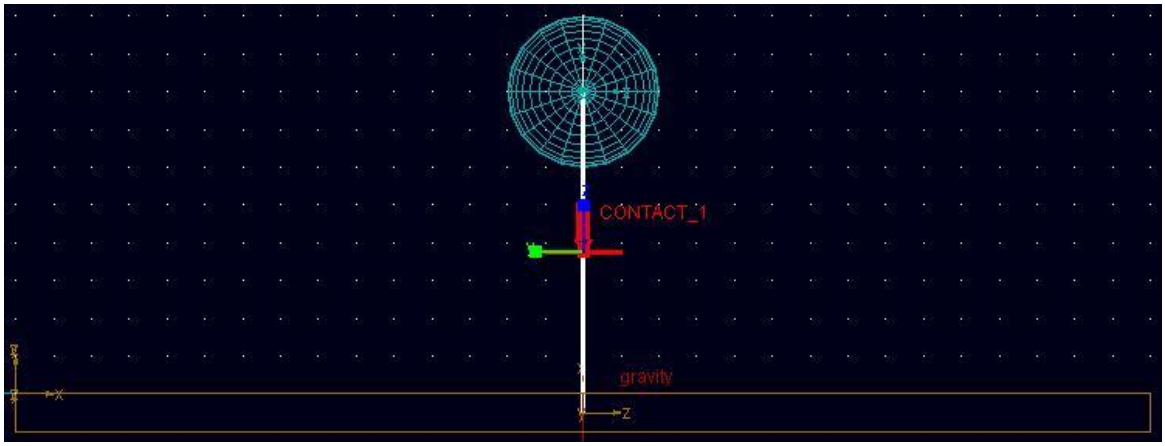

Figure 9: A sphere element (blue) falling and bouncing on a box element (brown)

3.2.1 IMPACT function:

Stiffness	1.0E+008
Force Exponent	2.2
Damping	1.0E+004
Penetration Depth	1.0E-004

Starting with a standard set of characteristics, the sphere's behaviour is discussed for different values of e. By doing so, the effect of this variable is illustrated. The time step used is 0.5ms, which appears accurate enough for this purpose. The unit of stiffness is N/m, force exponent is dimensionless, the unit of damping is $N \cdot s/m$ and that of the penetration depth is m.

In Appendix A, Figure 11, four different values of e are plotted, one of them being the standard 2.2. In this figure it can be seen that:

- Low values of e lead to rebounds and vibrations when the sphere is supposedly at rest.
- At high values of e, the sphere penetrates the floor, with increasing penetration depths.
- There is an optimal e at which no bouncing occurs.

Stiffness	1.0E+008
Force Exponent	1.1
Damping	1.0E+004
Penetration Depth	1.0E-004

To illustrate the effect of k, the stiffness variable, several situations with different values of k are plotted. The standard set is as can be seen be seen on the left, with a lower force exponent, e. By doing so, the effect of k is more easily visible.

In Appendix A, Figure 12, four different values of k are plotted. From the graphs it can be seen that:

- At low values of k, the sphere penetrates the floor, with increasing penetration depths.
- Increasing k leads to rebounds, with greater rebound heights for greater values of k.
- After an optimal k the rebound heights decrease again until no rebound occurs anymore.

Stiffness	1.0E+008
Force Exponent	1.1
Damping	1.0E+004
Penetration Depth	1.0E-004

The effects of c_{max} are plotted with the same low force exponent, e, of 1.1. Four different values of c_{max} are plotted, ranging from 1.0E+002 to 1.0E+005. The plots can be seen in Appendix A, Figure 13. From the graphs it can be seen that:

- Low values of c_{max} allow relatively large rebound heights.
- Increasing c_{max} rapidly leads to complete suppression of the rebounds.

Stiffness	1.0E+008
Force Exponent	1.1
Damping	1.0E+004
Penetration Depth	1.0E-004

The last of the four variables is the penetration depth, d. It is important to note that this depth does not represent the maximum penetration depth. It is the penetration depth at which the damping value is at maximum. So it is in an important relation to the user-specified damping value.

Appendix A, Figure 14, shows the behaviour for five different values of d. From the graphs it can be seen that:

- Very small values for d (1.0E-008 to 1.0E-004) show very little differences.
- Increasing d results in larger rebound heights, until a maximum is reached.

Stiffness	2.5125E+004
Force Exponent	1
Damping	0
Penetration Depth	1.0E-004

If damping is removed from the IMPACT function and the force exponent is set to 1, the contact should be perfectly elastic. To research this, the set of characteristics on the left was used and the stiffness was varied. In the case of perfect elasticity, the sphere would rebound up to 0.4 meters again.

In Appendix A, Figure 15, the rebound heights are plotted for seven different stiffness values. From the graphs it can be seen that:

- High stiffness values lead to small rebound heights and small maximum penetration depths.
- Low stiffness values lead to large rebound heights and large maximum penetration depths.
- The rebound height converges to 0.4 meters.
- The radius of the sphere determines the maximum penetration depth and thus the maximum rebound height. Lower stiffness values cannot be researched with this model.

An easier way to achieve perfect elasticity is the POISSON restitution method. Before discussing the findings above, the report continues with the POISSON restitution method.

3.2.2 POISSON restitution:

This method uses only two user-specified variables. First the value for the penalty is kept static and the behaviour is evaluated for several different values of COR (restitution coefficient). Then the value for COR is kept static and the behaviour is evaluated for several different values of p, the penalty. The time step used here is also 0.5ms. The unit of penalty is $N \cdot s/m$ and COR is dimensionless.

In Appendix A, Figure 16, eleven different values of COR are plotted. In this figure it can be seen that:

- COR = 1.0 does not lead to energy conservation, because k is believed to be too low.
- Decreasing the COR value leads to an increase of energy dissipation.
- COR = 0.0 leads to 100% energy dissipation.

Now COR is kept static at 0.7 and the sphere's behaviour is evaluated for several different values for the penalty.

In Appendix A, Figure 17, ten different values of p are plotted. In this figure it can be seen that:

- When p is too low, the sphere sinks through the floor or the collision simply does not occur.
- The higher p is, the better the sphere follows the expected behaviour based on COR.
- When p is too high, an unexpected rebound can occur when the sphere is supposedly at rest.

The report will now continue with a discussion about all the findings above.

3.2.3 Discussion:

In the following paragraphs the findings from the previous pages are discussed. The order of the variables in this discussion is the same as on the previous pages.

From the theory we know that the force exponent e in the IMPACT function is a measure of the non-linearity of the spring component. It is recommended to use values of $e > 1$. It was seen that values of $0 < e < 1$ create unexpected vibrations, which is due to the relatively high spring force even at small penetration depths. The recommended values of $e = 1.1$ for rubbers, $e = 1.5$ for soft metals and $e = 2.2$ for harder metals appear to be plausible. For high values, for example $e = 5.0$, the spring force is too small at small penetration depths and thus the sphere will sink through the floor. It is recommended to use values between 1.1 and 2.2, depending on the choice of materials.

On the subject of the stiffness we know from the theory that it is based on material and geometrical properties. From the graphs it could be seen that when k is too low, the spring force is insufficient to keep the sphere from sinking. When k is too high, the contact is obviously too stiff and the sphere will come to an instant stop. It was also observed that there is an optimal value for k. For this model is was $k = 1.0 \cdot 10^8\ N/m$. The stiffness variable will be further researched in later cases.

The damping depends on two variables, the maximum damping variable, c_{max}, and the penetration depth, d. A high maximum damping will lead to (almost) completely damped out rebounds. Decreasing c_{max} allows rebounds to occur. Decreasing c_{max} even further allows larger rebound heights, until the rebound height converges to a maximum at $c_{max} = 0$. The actual damping value ramps up from zero to c_{max} over a distance specified by d. For high values of d the rebounds appear to be less damped than in the case of low values of d. Especially when d is larger than the actual maximum penetration depth, the work done by the damping force is significantly smaller than for smaller d values. When less work is done by the damping force, the rebounds will appear less damped, which corresponds with the results in the graphs.

When the maximum damping is set to zero and the force exponent is set to one, the IMPACT function will act as a linear spring. Perfect elasticity was expected, but it appears that a large penetration depth is needed to achieve this. Since penetration depths should be relatively small in order for the model to be realistic, the IMPACT function appears unsuitable for perfectly elastic contacts. The POISSON restitution model is preferred for (near) perfectly elastic contacts.

The two user-specified variables in the POISSON restitution method are the COR (coefficient of restitution) and the penalty. The COR is a measure of the energy conservation. According to the theory, the sphere would rebound all the way up with a COR value of 1. This does not happen in the graph, because the penalty value is not high enough. The higher the penalty value, the more accurate the rebounds are. This comes at an expense, which can be seen in Figure 17 after $\sim 1.6\ s$. Suddenly unexpected rebounds can occur. This is because the high penalty value can create large normal forces, even when the sphere is supposedly resting on the floor. When the penalty value is far too low, the normal force cannot support the sphere at all. From this it can be concluded that the POISSON restitution method requires the user to choose the penalty value carefully.

Both normal force calculation methods have been evaluated and discussed in this case of the bouncing ball. This case does not include frictional forces. These will be covered in the next case.

3.3 Rolling ball (2D)

In the second case the behaviour of a sphere, with an infinite stiffness, rolling on a plane is observed. Even though the movement is purely horizontal, the normal force cannot be excluded. The frictional force depends on the normal force. This case first researches the compatibility of several normal force options with the Coulomb friction model. One specific option will be chosen with which the Coulomb friction model will be researched.

To illustrate what the different variables of the Coulomb friction model do, the X-coordinate of the sphere's center-of-mass and its second derivative (the acceleration along the X axis) is analysed. From the theory it is known that when there is no slip (meaning that there is no relative velocity between the sphere and the floor), the frictional force is zero. A non-zero relative velocity produces a frictional force and so the sphere will converge to a no-slip situation. Therefore the sphere is not given an initial translational velocity, but an initial angular velocity. By doing so, the behaviour of the sphere can be observed while it converges to a no-slip situation. The initial conditions are:

$x_0 = 0\,m$
$\theta_0 = -1000\ degrees/s$ (the minus sign makes this rotation clockwise)

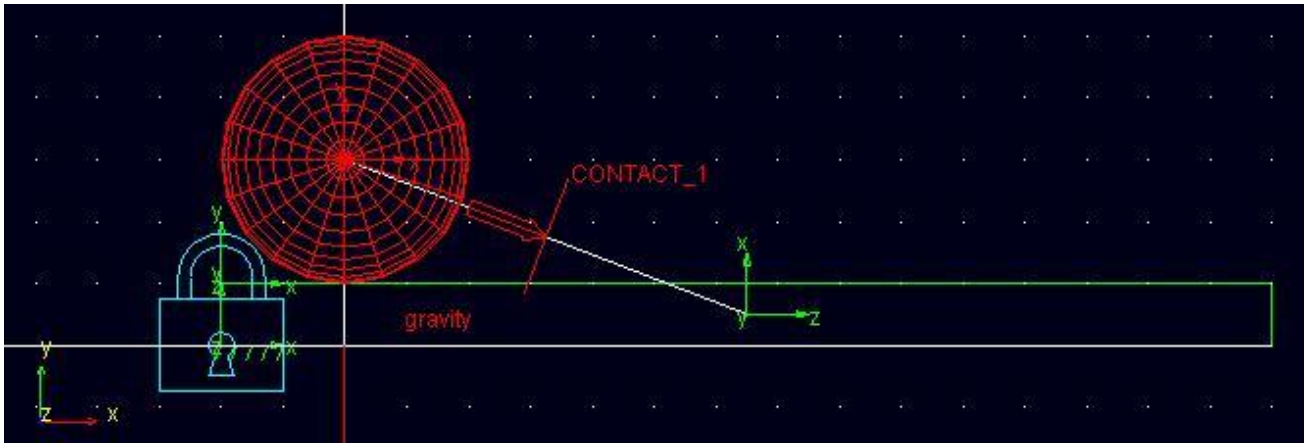

Figure 10: A sphere element (red) first slipping and then rolling on a box ement (green)

3.3.1 Suitable normal force configuration

Since the sphere is touching the floor throughout the whole simulation, a constant normal force is expected. Oscillations in the normal force will affect the frictional force, as these oscillations will also occur in the frictional force. So the criterion for the normal force configuration is that the resulting normal force is more or less constant.

The IMPACT function acts as a mass-spring-damper system and calculates a normal force that is constant when the sphere is in a vertical equilibrium at a specific penetration depth. Because of this, the Y-coordinate of the sphere will oscillate at the start of the simulation and it will reach equilibrium after a period of time. The length of this period depends on the user-specified variables in the IMPACT function and the time step of the simulation. So the criterion is that the normal force is more or less constant before the relative velocity nears the friction transition velocity.

For several configurations of the IMPACT function, the Y-coordinate was plotted. The graph containing these plots can be found in Appendix B, Figure 19. The time step used is 0.5ms. From the graph it can be seen that lowering the force exponent, *e*, to 1.1 provides us a normal force that appears to be suitable for this case, so that the effect of the variables in the Coulomb friction model can be illustrated.

The POISSON restitution model is an alternative to the IMPACT function model, so it was also tested. In Appendix B, Figure 18, it can be seen that the calculated normal force was far from constant. The plots of the Y-coordinate are governed by vibrations, with COR=0.0 being an exception. This exception does lead to discontinuities in the sphere's acceleration and thus is not ideal for illustrating the Coulomb friction model's variables.

Upcoming research on the Coulomb friction model will be done with the following normal force configuration:

Normal Force	Impact
Stiffness	1.0E+008
Force Exponent	1.1
Damping	1.0E+004
Penetration Depth	1.0E-004

3.3.2 Coulomb friction model

Static Coefficient	0.3
Dynamic Coefficient	0.1
Stiction Transition Vel.	0.1
Friction Transition Vel.	1.0

All the following simulations will be performed with the normal force configuration stated on the previous page. Starting with a standard set of characteristics, the sphere's behaviour is discussed for different values of μ_s, the static coefficient. By doing so, the effect of this variable is illustrated. The time step used is 0.5ms, which appears accurate enough for this purpose, and is used throughout all the upcoming simulations in this model. The static and dynamic coefficient are dimensionless and the transition velocities have the unit m/s.

In Appendix B, Figure 21, the displacement in the X-direction is plotted for six different values of μ_s, one of them being the standard 0.3. In this figure it can be seen that:

- The parabolic start of the plots is the same for all values of μ_s.
- The transition from the parabolic domain to the linear domain is differs per value of μ_s.
- In all cases (except $\mu_s = 0$, which is an unrealistic value) the plots in the linear domain are parallel, meaning that all values of μ_s lead to the same velocity in the X-direction.

In Appendix B, Figure 20, the acceleration in the X-direction is plotted for the same six different values of μ_s. In this figure it can be seen that:

- During the first milliseconds, the normal force approaches an equilibrium, creating vibrations in the frictional force and thus acceleration. This also occurs in the other simulations of this model.
- At first, the acceleration is constant and the same for all values of μ_s, hence the shared parabolic domain in the previous graph.
- When the contact point's relative velocity decreases and reaches the friction transition velocity, the acceleration increases to a maximum value that is $\mu_s \cdot 9.81$. The duration of this increase is shorter for higher values of μ_s.
- After reaching a maximum, the acceleration quickly drops to zero.

Static Coefficient	0.3
Dynamic Coefficient	0.1
Stiction Transition Vel.	0.1
Friction Transition Vel.	1.0

The other efficient in Adams that is user-specified is the dynamic coefficient. Starting with the same standard set of characteristics, the sphere's behaviour is discussed for different values of μ_d.

In Appendix B, Figure 23, the displacement in the X-direction is plotted for five different values of μ_d, one of them being the standard 0.1. In this figure it can be seen that:

- The parabolic start of the plots differs for every different value of μ_d.
- In all cases (except $\mu_d = 0$, which is an unrealistic value) the final velocity is the same.
- $\mu_d = 0$ never reaches the stiction transition velocity, since its initial friction force is zero and does not change.

In Appendix B, Figure 22, the acceleration in the X-direction is plotted for the same five different values of μ_d. In this figure it can be seen that:

- At first, the acceleration is constant, but not the same for the different values of μ_d.
- The constant acceleration is shorter for higher values of μ_d. Except for $\mu_d = 0.3$, which is a special case since $\mu_d = \mu_s$.

- When the contact point's relative velocity decreases and reaches the friction transition velocity, the acceleration increases (or decreases for $\mu_d > \mu_s$) to a (maximum) value that is $\mu_s \cdot 9.81 = 0.3 \cdot 9.81$. The duration of this increase is shorter for higher values of μ_d.
- After reaching this maximum, the acceleration quickly drops to zero. The duration of this decrease is the same for all values of μ_d.

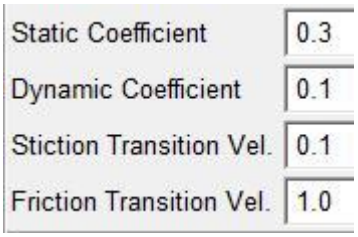

Now that the coefficients have been researched, the transition velocities remain. First the friction transition velocity, V_d, will be varied while the other variables have the same static values presented on the left of this text.

In Appendix B, Figure 25, the displacement in the X-direction is plotted for six different values of V_d. In this figure it can be seen that:

- The parabolic start of the plots is the same for all values of V_d, but extends further for lower values of V_d.
- In all cases the plots in the linear domain are parallel, meaning that all values of μ_s lead to the same velocity in the X-direction.

In Appendix B, Figure 24, the acceleration in the X-direction is plotted for the same six different values of V_d. In this figure it can be seen that:

- At first, the acceleration is constant and the same for all values of V_d. Lower values of V_d have a longer constant acceleration, hence the extended parabolic domain in the previous graph.
- The maximum acceleration is the same for all values of V_d, namely $\mu_d \cdot 9.81$. The duration of the increase towards this value is longer for higher values of V_d.
- The decrease from this maximum acceleration to zero is the same for all values of V_d.

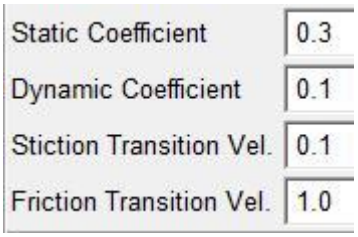

The other transition velocity is the stiction transition velocity, V_s. In Appendix B, Figure 27, the displacement in the X-direction is plotted for eight different values of V_s, including two values when $V_s > V_d$. In this figure it can be seen that:

- When $V_s \leq V_d$ the parabolic domain is the same. When $V_s > V_d$ the parabolic domain is shorter.
- Just like in the previous cases, the final velocity is the same for all values.

In Appendix B, Figure 26, the acceleration in the X-direction is plotted for the same eight different values of V_s. In this figure it can be seen that:

- At first, the acceleration is constant and the same for all values of V_s. The length of this constant acceleration is the same for $V_s \leq V_d$, but is shortened for $V_s > V_d$.
- All values lead to the maximum of $\mu_s \cdot 9.81$. The duration of this ramp-up is shorter for higher values of V_s. When $V_s \geq V_d$, this ramp-up is instanteous.
- After reaching the maximum, all plots drop back to zero and share a common intersection point. Only the graphs for $V_s > V_d$ do not share this common intersection point.

The report will now continue with a discussion about all the findings above.

3.3.3 Discussion:

In the following paragraphs the findings from the previous pages are discussed. The order of the variables in this discussion is the same as on the previous pages.

When varying μ_s it was noticed that during the first 0.22 seconds the sphere's behaviour was the same for all values of μ_s, which is logical, because μ_d and V_d are equal in all cases. It is when the relative contact velocity drops below V_d when the different cases start to act differently. Since $\mu_d = 0.1$, the sphere's acceleration is initially $9.81 \cdot 0.1 \approx 1\ m/s^2$, and for different values of μ_s the acceleration increases (only for $\mu_s > \mu_d$, of course) to a peak value $9.81 \cdot \mu_s$. Since V_s is the same in all cases, these peaks are all at the same velocity, V_s. Then why do these peaks occur at different times? It is evident that the coefficient of friction has a steeper incline for higher values of μ_s at a constant V_s (review Figure 7 if this is unclear). Therefore the frictional force increases faster for higher values of μ_s, decreasing the relative contact velocity faster for higher values of μ_s and thus making the acceleration increase towards the spike steeper for higher values of μ_s. And since the frictional force is higher at velocity V_s for higher values of μ_s, the contact velocity drops down to zero faster and so does the acceleration. When the acceleration has reached zero, the final velocity is constant and the same for all values of μ_s. The parallel plots in Figure 21 show that the final velocities are the same indeed. Values of $\mu_s \leq \mu_d$ lead to incorrect sphere behaviours according to the theory of Chapter 2.8.

When varying μ_d it was noticed that the sphere's acceleration starts at different values, which can be explained by the simple fact that the acceleration is $9.81 \cdot \mu_d$ for contact velocities that are greater than V_d, which is the case at the start of the simulation. Higher values of μ_d lead to higher frictional forces and thus the velocity reaches V_d earlier, at which the coefficient of friction starts changing from μ_d to μ_s. Since μ_s is the same in all simulations, the sphere's acceleration peaks at the same value. When $\mu_d = \mu_s$, the change in coefficient of friction is equal to zero. When $\mu_d = 0$ the contact velocity remains constant and thus the friction and stiction transition velocities are never reached. The change from μ_d to μ_s is shorter in time for higher values of μ_d, because then the contact velocity V_d is reached faster. After the peak, the acceleration drops to zero at the same rate for all values of μ_d, since that rate depends on μ_s and V_s only. Again the final velocity is the same for all values of μ_d. When $\mu_d \geq \mu_s$ or $\mu_d = 0$ the sphere's acceleration is incorrect according to the theory of Chapter 2.8.

When varying V_d it was noticed again that the sphere's acceleration is constant and the same for all simulations. A higher value for V_d means that the friction transition velocity is reached earlier, so the increase in the acceleration starts earlier. All simulations have the same value for V_s, which occurs at the peaks of all plots. When the difference between these two transition velocities becomes smaller, the change in acceleration becomes more rapidly, or even instant when $V_d = V_s$. After the peak, the acceleration drops down to zero at the same rate for all values of V_d, since this rate only depends on μ_s and V_s. Again the final velocity is the same for all values of V_d. When $V_d = 0$ the sphere's acceleration is incorrect according to the theory of Chapter 2.8. In fact, $V_d = 0$ cannot be modeled.

The last variable that was varied was V_s. Since μ_s and μ_d are the same in all simulations, the acceleration is the same at the start and at the peaks. When $V_s = V_d$ the acceleration instantly jumps to $9.81 \cdot \mu_s$ when the contact velocity reaches V_s. When $V_s > V_d$ the jump in the acceleration occurs earlier and the friction transition velocity V_d is completely disregarded. For values of V_s that are greater than V_d, which agrees with the theory of Chapter 2.8, the difference between V_s and V_d determines the rate of climb from μ_d to μ_s.

Since the values of V_s are different in the different simulations, the decrease from μ_s to zero is not the same in all plots. Like in all other simulations, the final velocity is constant and the same for all values of V_s.

The four sets of simulations show us several things. We now know how the sphere's acceleration and travelled distance are affected by varying the four variables μ_s, μ_d, V_s and V_d. Since the acceleration is expected to be continuous, values for which a jump in the acceleration graph is created, are not recommended. This excludes the values $V_d \leq V_s$. The transition velocities are supposed to be non-zero: $V_s > 0 \ \wedge \ V_d > 0$. To follow the theory of Chapter 2.8, the coefficients of friction also have to be within a certain range. The excluded values are: $\mu_s = 0 \ \wedge \ \mu_d = 0 \ \wedge \ \mu_s \leq \mu_d$.

4. Recommended values:

4.1 Introduction

In Chapter 3 the variables of the IMPACT function model, the POISSON restitution model and Coulomb friction model were analyzed and discussed with the use of two Adams models. Now that we know how these models work and what effects the variables have on the contact behaviour, we want to know what values are suitable for Adams models that resemble real-life constructions.

Chapter 4.2 will discuss the recommended values for the IMPACT function model, Chapter 4.3 will discuss the recommended values for the POISSON restitution model and in Chapter 4.4 the recommended values for the Coulomb friction model are discussed.

4.2 IMPACT function model

In this model there are four variables, namely stiffness k, the force exponent e, the maximum damping c_{max} and the penetration depth d. These four parameters are discussed in this order in the following paragraphs.

4.2.1 Stiffness k:

Even though the name *stiffness* might sound like it is a material property, it is not just that. It also depends on the geometry of the colliding objects. Therefore there is no handbook for choosing the value for k. The best option is to do multiple simulations in Adams with different values of k to determine the optimal value, the value at which the Adams contact behaviour resembles the real world contact behaviour. Some organizations that use Adams develop experience with the IMPACT function and its parameters, for their specific applications.[10]

Since this study does not include extensive research like the aforementioned organizations do, we hardly have any grip on what is a realistic value for the stiffness parameter. Adams includes a standard value for the stiffness when initially setting up a contact between two objects, though. This value is $1.0 \cdot 10^8\ N/m$. Because of this, it is expected that a realistic value of k would be in the range of $1.0 \cdot 10^7\ N/m$ to $1.0 \cdot 10^9\ N/m$.

4.2.2 Force exponent e:

The force exponent is a measure of the non-linearity of the IMPACT function's spring force. In Chapter 2.6 it was already explained that the recommended value is $e > 1$, because lower values will lead to discontinuities when IMPACT activates. The actual value of e is a material property[11]. Soft materials, like rubbers, have a force exponent of $e \approx 1.1$. For harder materials, the force exponent increases. Soft metals, like aluminium, have a force a force exponent of $e \approx 1.5$ and hard metals, like steel, have a force exponent of $e \approx 2.2$. It is not recommended to use higher values, which was evaluated in Chapter 3.2.1.

4.2.3 Maximum damping c_{max}:

Some sources say that it is recommended to have a maximum damping coefficient that is 1% of the stiffness value[12]. Experienced users believe that c_{max} should be even smaller. In Adams, the standard stiffness is $1.0 \cdot 10^8\ N/m$ and the standard maximum damping coefficient is $1.0 \cdot 10^4\ N \cdot s/m$, which is 0.01% of the stiffness value. The best option is to do multiple simulations in Adams with different values of c_{max} to determine the optimal value, the value at which the Adams contact behaviour resembles the real world contact behaviour.

4.2.4 Penetration depth d:

This penetration depth is not the maximum penetration depth, but the measure of how the damping coefficient ramps up from zero to c_{max}. The value should be smaller than the expected maximum penetration depth. A reasonable value for this parameter is $0.01\ mm$.[13]

To conclude Chapter 4.2: the IMPACT function works well as a method for calculating the normal force during a collision, but determining the correct values can take extra research time, because of the geometry dependency of the parameters.

---

[10] Chris Verheul, 'Contact Modeling' presentation, sheet 10; http://www.insumma.nl/wp-content/uploads/SayField_Verheul_ADAMS_Contacts.pdf
[11] Chris Verheul, 'Contact Modeling' presentation, sheet 11; http://www.insumma.nl/wp-content/uploads/SayField_Verheul_ADAMS_Contacts.pdf
[12] Chris Verheul, 'Contact Modeling' presentation, sheet 13; http://www.insumma.nl/wp-content/uploads/SayField_Verheul_ADAMS_Contacts.pdf
[13] Chris Verheul, 'Contact Modeling' presentation, sheet 12; http://www.insumma.nl/wp-content/uploads/SayField_Verheul_ADAMS_Contacts.pdf

4.3 POISSON restitution model

In this model there are two variables, namely the coefficient of restitution COR and the penalty parameter p. These two parameters are discussed in this order in the following paragraphs.

4.3.1 Coefficient of Restitution $\boldsymbol{COR}$:

This parameter defines a continuum between a perfectly elastic (COR = 1.0) and perfectly inelastic (COR = 0.0) collision. These two perfect instances will never occur in real life, because the energy dissipation during a collision will always be partial. In Appendix C, Table 1, a list of values for COR can be found. The table is extracted from Adams/Solver documentation and lists 34 different combinations of materials. For each combination a value for COR is given. In the table the values range from 0.65 to 0.95. When choosing the POISSON restitution model, determining the correct value of the coefficient of restitution is fairly simple, by using the table in Appendix C or different sources.

4.3.2 Penalty $\boldsymbol{p}$:

In the POISSON restitution model the COR is the most important parameter, but the penalty parameter should not be forgotten. From Chapter 3.2.2 we learned how the penalty parameter affects the contact behaviour. When the penalty is too low, the normal force is not sufficient. When the penalty is too high, the normal force can become non-zero when it is expected to be zero, due to numerical integration issues. Adams' standard value for the penalty parameter is $p = 1.0 \cdot 10^8$. Since integration issues are easily spotted (note the random rebounds), the penalty can be increased until these integration issues arise. The most preferred value for the penalty parameter is the highest value that does not cause integration issues.

To conclude Chapter 4.3: the POISSON restitution model is a great method for calculating the normal force when the energy loss during a collision is known. The penalty parameter would have to be infinite for it to be ideal, but that would lead to integration issues, too. Therefore, regardless of the value of COR, the penalty parameter should be $p = 1.0 \cdot 10^8$ or greater if possible.

4.4 Coulomb friction model

In this model there are four variables, namely the two coefficients of friction, μ_s and μ_d, and the two transition velocities, V_s and V_d. These four parameters are discussed in this order in the following paragraphs. For reference it is advised to review Figure 7.

4.4.1 Coefficient of friction $\boldsymbol{\mu_s}$ and $\boldsymbol{\mu_d}$:

When the contact velocity is between zero and the stiction transition velocity, the coefficient of friction ramps up from zero to the static coefficient of friction μ_s. This coefficient is a material property, it depends on the two materials of the objects in contact. For contact velocities between the stiction transition velocity and the friction transition velocity, the coefficient of friction decreases from μ_s to μ_d, the dynamic coefficient of friction. It is unusual for μ_d to be greater than μ_s, which can be seen in Appendix C. In that appendix, in Table 1, μ_s and μ_d are listed for 34 different combinations of materials. In the table the values are very wide-spread. So whenever an Adams model needs Coulomb friction to be implemented, the choice of materials is very important, since it determines the static coefficient of friction μ_s and dynamic coefficient of friction μ_d.

For both μ_s and μ_d the recommended values can be found by using the table in Appendix C or other sources. If the specific combination of materials is not in the table, remember that $\mu_s > \mu_d$ when choosing your own values.

4.4.2 Transition velocity $\boldsymbol{V_s}$ and $\boldsymbol{V_d}$:

To determine what the recommended values are for both transition velocities V_s and V_d, we combine knowledge from Chapters 2.5 and 2.8. In reality, the coefficient of friction instantly jumps from zero to μ_s at contact velocity zero. This effect is known as stiction. Adams models this discontinuity as a continuity, seen in Figure 7. Now the discontinuity at zero velocity is spread over a velocity range between zero and V_s, making the coefficient of friction a continuous function of the contact velocity. Even though stiction is not supported by Adams, the effect can be approached by making V_s approach zero. The standard value in Adams is $0.1\ m/s$. From Chapter 3.3.2 we know that this value can be increased, as long as its value remains lower than V_d.

When the contact velocity is equal to or greater than V_d, the coefficient of friction remains constant at μ_d. Like stated above, the friction transition velocity should be greater than the stiction transition velocity. The standard value in Adams is $1.0\ m/s$.

In SolidWorks/COSMOSMotion[14] the standard transition velocities for a contact between two dry steel objects are $V_s = 0.1\ mm/s$ and $V_d = 10\ mm/s$. This program uses a similar Coulomb friction model. When comparing the standard values of Adams and the standard values of SolidWorks, it appears that the actual choice for the transition velocities is very open to the end-user of the program.

To conclude Chapter 4.4: the Coulomb friction model is a great method for calculating the frictional force. Even though stiction cannot be modeled, by choosing a low value for V_s, the phenomenon of stiction can be approached. The two known values of the coefficient of friction, μ_s and μ_d, are material properties and can be found in Appendix C or other sources. The transition velocities are free to the user to choose, with V_s being close to zero and smaller than V_d.

[14] Kxcad, Understanding Contact Friction, http://www.kxcad.net/solidworks/COSMOSMotion/usingmotionentities/constraints/contactconstraints/understanding_contact_friction.htm

5. Conclusion:

In this study it was researched how the contact models in MSC Adams are derived from Hertzian contact theory and other theories, how they are implemented in MSC Adams, what effect their parameters have on the contact behaviour and what the recommended values are for these parameters.

The first contact method is the IMPACT function model. The IMPACT function creates a normal force that consists of a spring force, which is derived from Hertzian contact theory, and a damping force, which is an Adams addition. This method includes four user-specified parameters. Their effect on the contact behaviour and the recommended values are discussed in Chapters 3.2.1, 3.2.3 and 4.2. The IMPACT function works well as a method for calculating the normal force during a collision, but determining the correct values can take extra research time, because of the geometry dependency of the parameters.

The second contact method is the POISSON restitution model. This method calculates a normal force based on the coefficient of restitution and a penalty parameter. For every combination of two colliding materials there is a certain value of the coefficient of restitution, which defines the energy loss during the collision. COR = 1.0 means no energy is lost, COR 0.0 means all energy is lost. The effect of the two user-specified parameters on the contact behaviour and the recommended values of these parameters are discussed in Chapters 3.2.2, 3.2.3 and 4.3. The POISSON restitution model is a great method for calculating the normal force when the energy loss during a collision is known. The penalty parameter would have to be infinite for it to be ideal, but that would lead to integration issues, too. Therefore, regardless of the value of COR, the penalty parameter as great as possible, without leading to integration issues.

The third contact method is the Coulomb friction model. This is a method for the optional frictional force. Real-life friction also includes stiction, which is the frictional force when the contact velocity is zero. Adams does not model this phenomenon. This method includes four user-specified parameters. Two of those, the coefficients of friction, are material properties and can be found in tables. The other two parameters are more open to the user to determine. The effect of the four parameters on the contact behaviour and the recommended values of these parameters are discussed in Chapters 3.3.2, 3.3.3 and 4.4. The Coulomb friction model is a great method for calculating the frictional force. Even though stiction cannot be modeled, by choosing a low value for V_s, the phenomenon of stiction can be approached. The two known values of the coefficient of friction, μ_s and μ_d, are material properties and can be found in Appendix C or other sources. The transition velocities are free to the user to choose, with V_s being close to zero and smaller than V_d.

Now that all three contact methods are discussed, we have a clear view of how they are to be used in Adams models. In the next and last chapter recommendations will be made for further research in relation to MSC Adams.

6. Recommendations:

For further studies on the subject of contact in MSC Adams some recommendations are made:

- To get a better insight in the parameters of the IMPACT function, it is recommended to build physical models and model these in MSC Adams. By then comparing the Adams models with the physical models, the ideal values for the parameters can be determined for these models.
- From Chapter 3.3.2 we have seen that the rolling ball always ends with the same final velocity. So in this case there is no rolling resistance. A research on rolling resistance in MSC Adams is recommended. Taking a look into Adams/Car is a possibility.

Appendix A (Bouncing Ball Graphs):

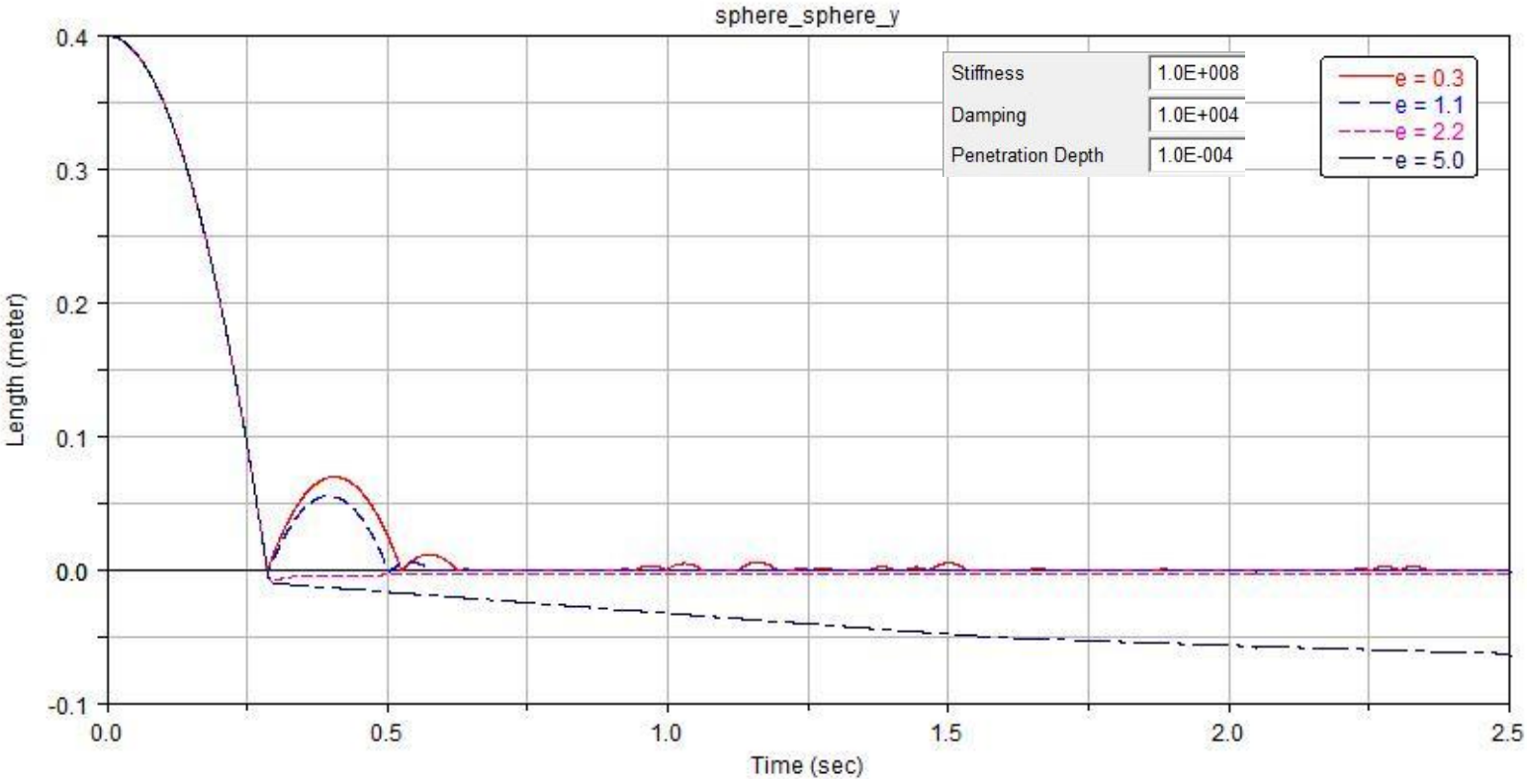

Figure 11: Graphs of the Y-coordinate of the sphere's CoM for 4 different force exponents.

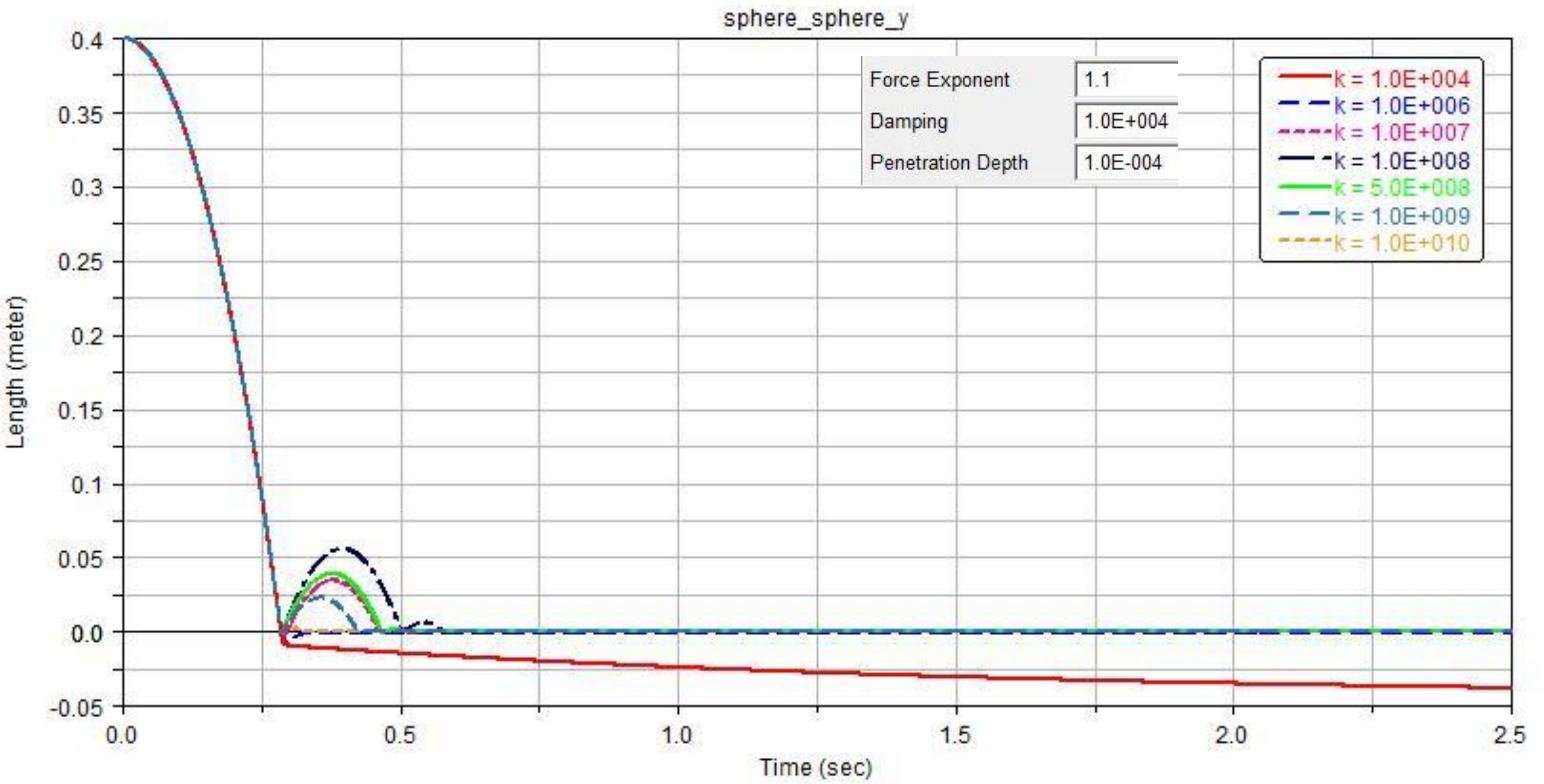

Figure 12: Graphs of the Y-coordinate of the sphere's CoM for 7 different stiffnesses.

Appendix A (Bouncing Ball Graphs - Continued):

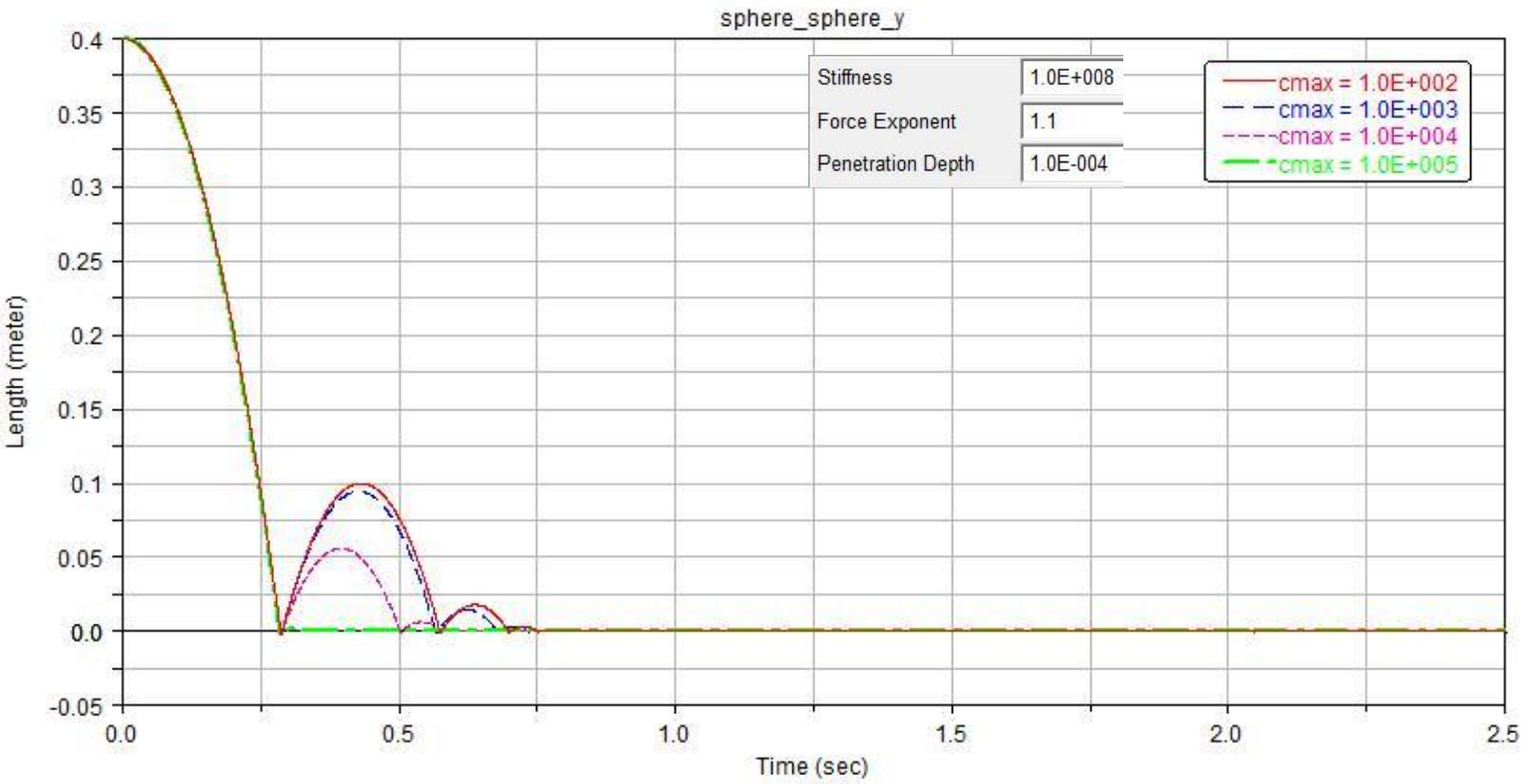

Figure 13: Graphs of the Y-coordinate of the sphere's CoM for 4 maximum dampings.

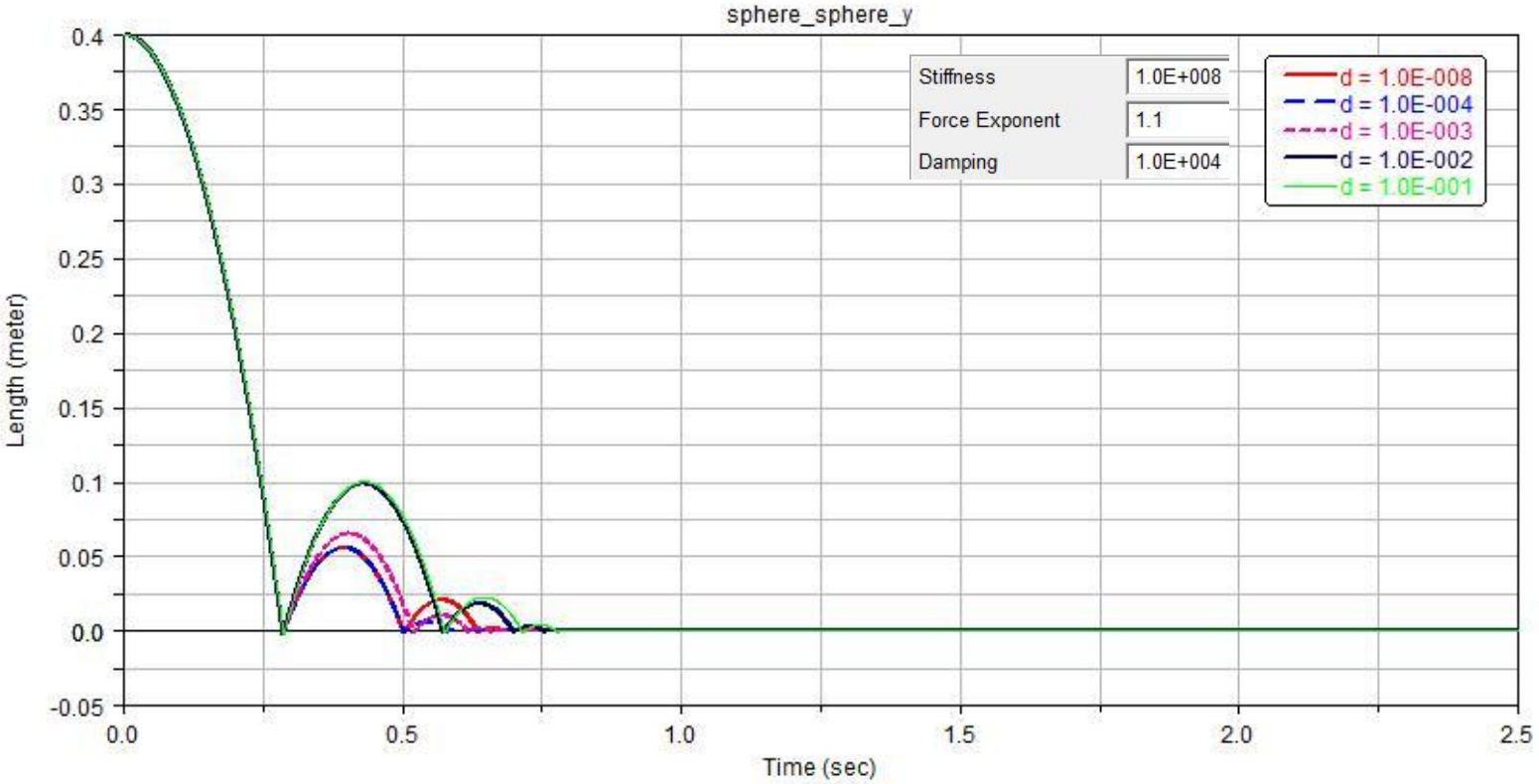

Figure 14: Graphs of the Y-coordinate of the sphere's CoM for 5 different penetration depths.

Appendix A (Bouncing Ball Graphs - Continued):

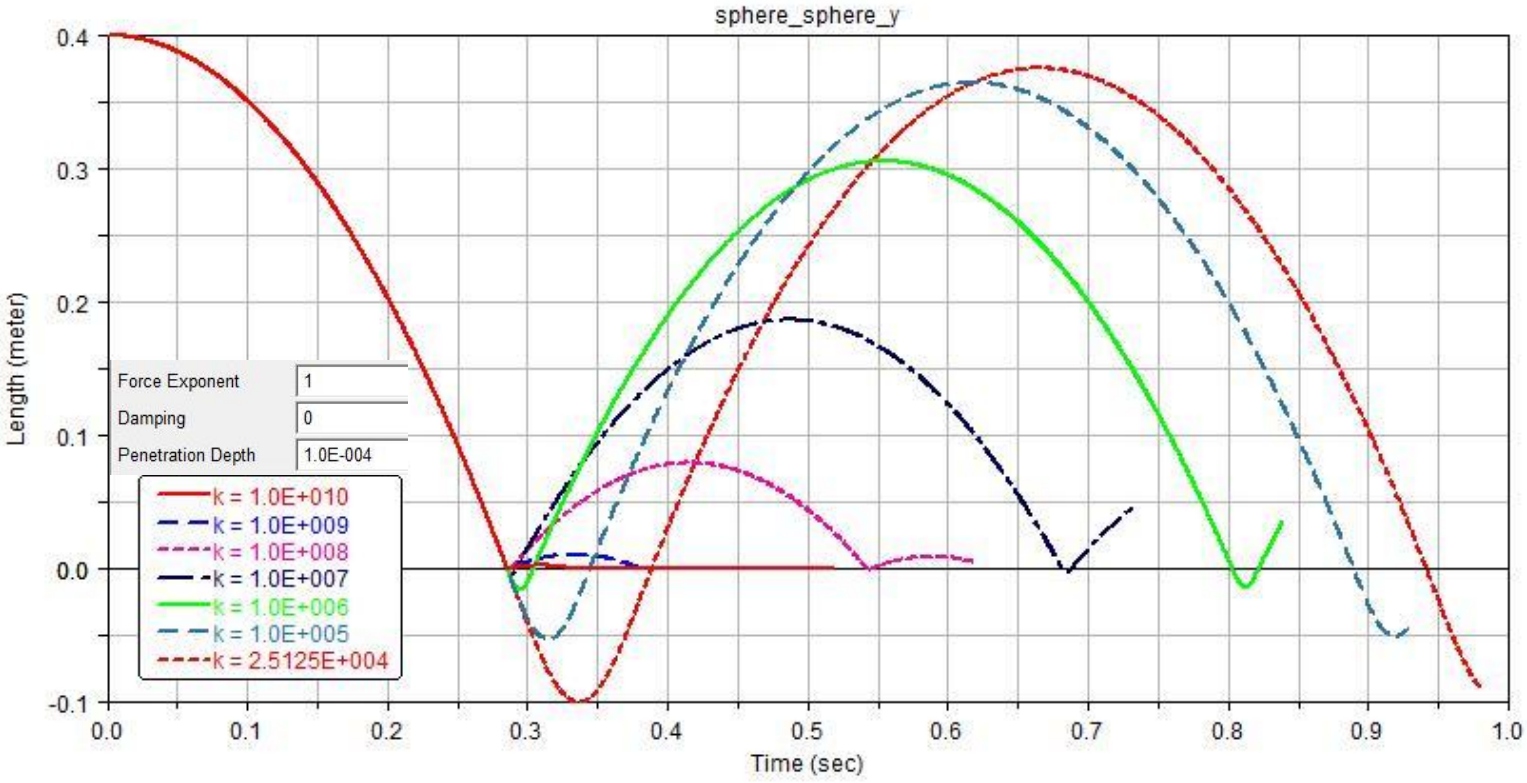

Figure 15: Graphs of the sphere's Y-coordinate for 7 stiffnesses, striving for perfect elasticity.

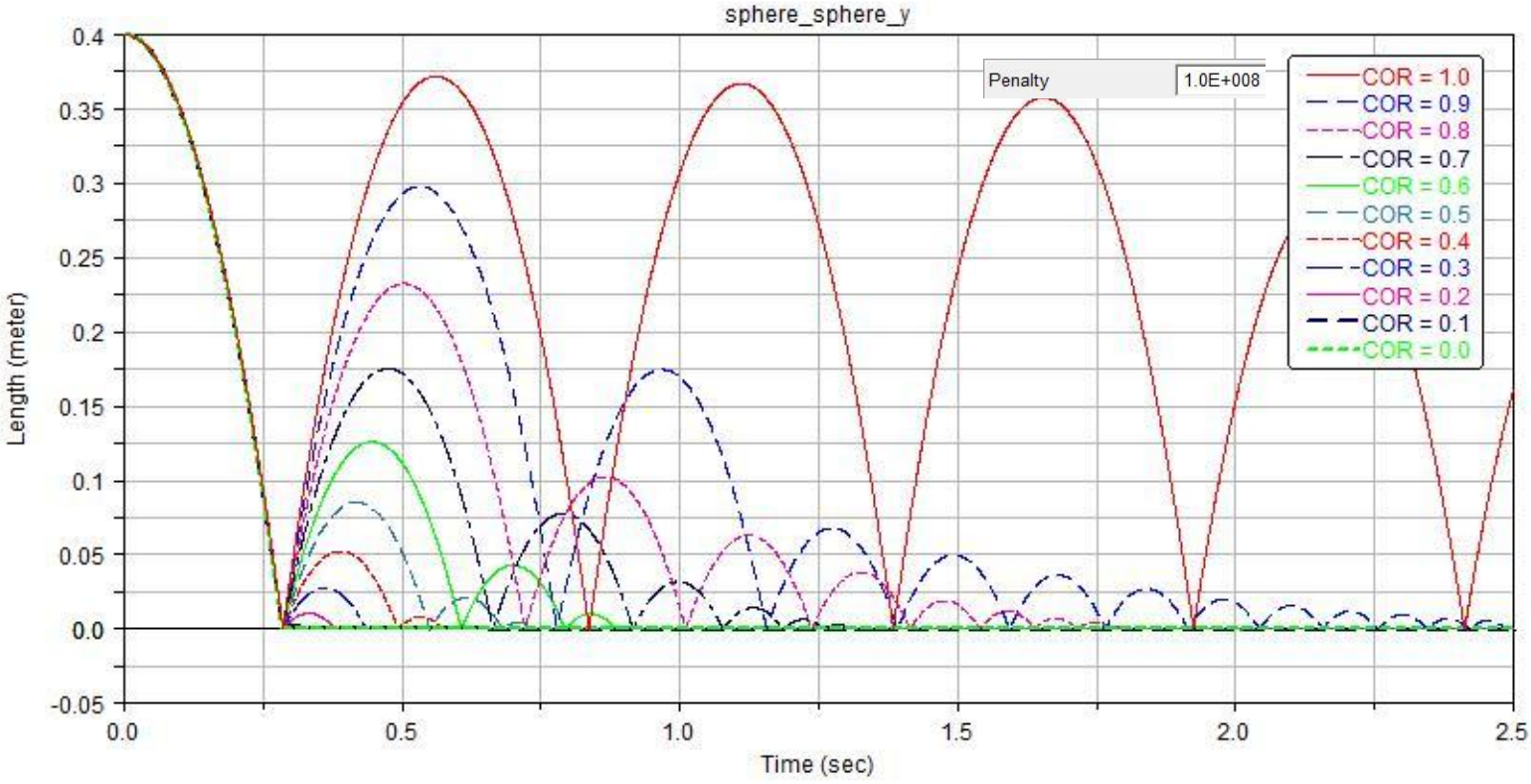

Figure 16: Graphs of the Y-coordinate of the sphere's CoM for 11 different COR´s.

Appendix A (Bouncing Ball Graphs - Continued):

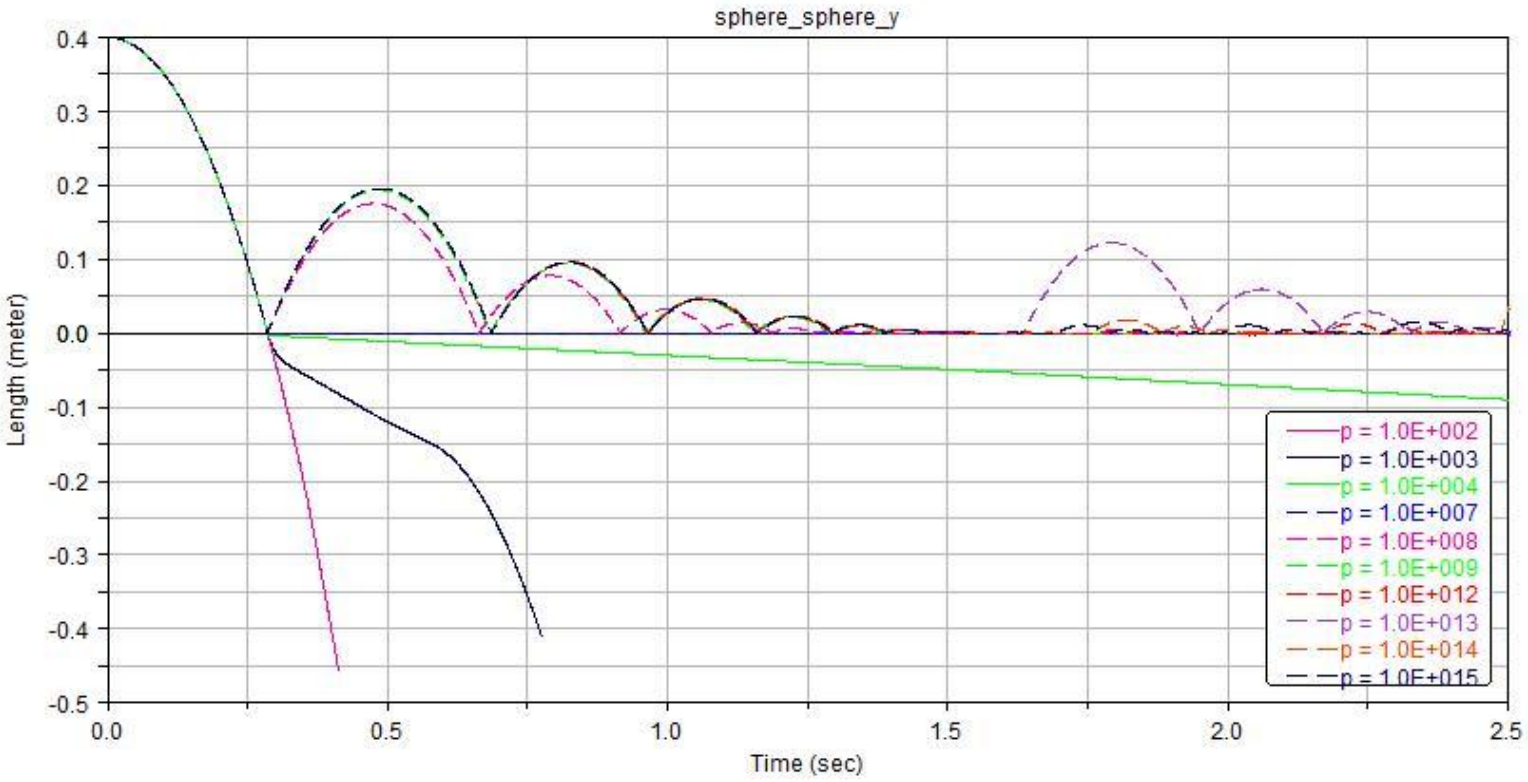

Figure 17: Graphs of the Y-coordinate of the sphere's CoM for 10 different penalties.

Appendix B (Rolling Ball Graphs):

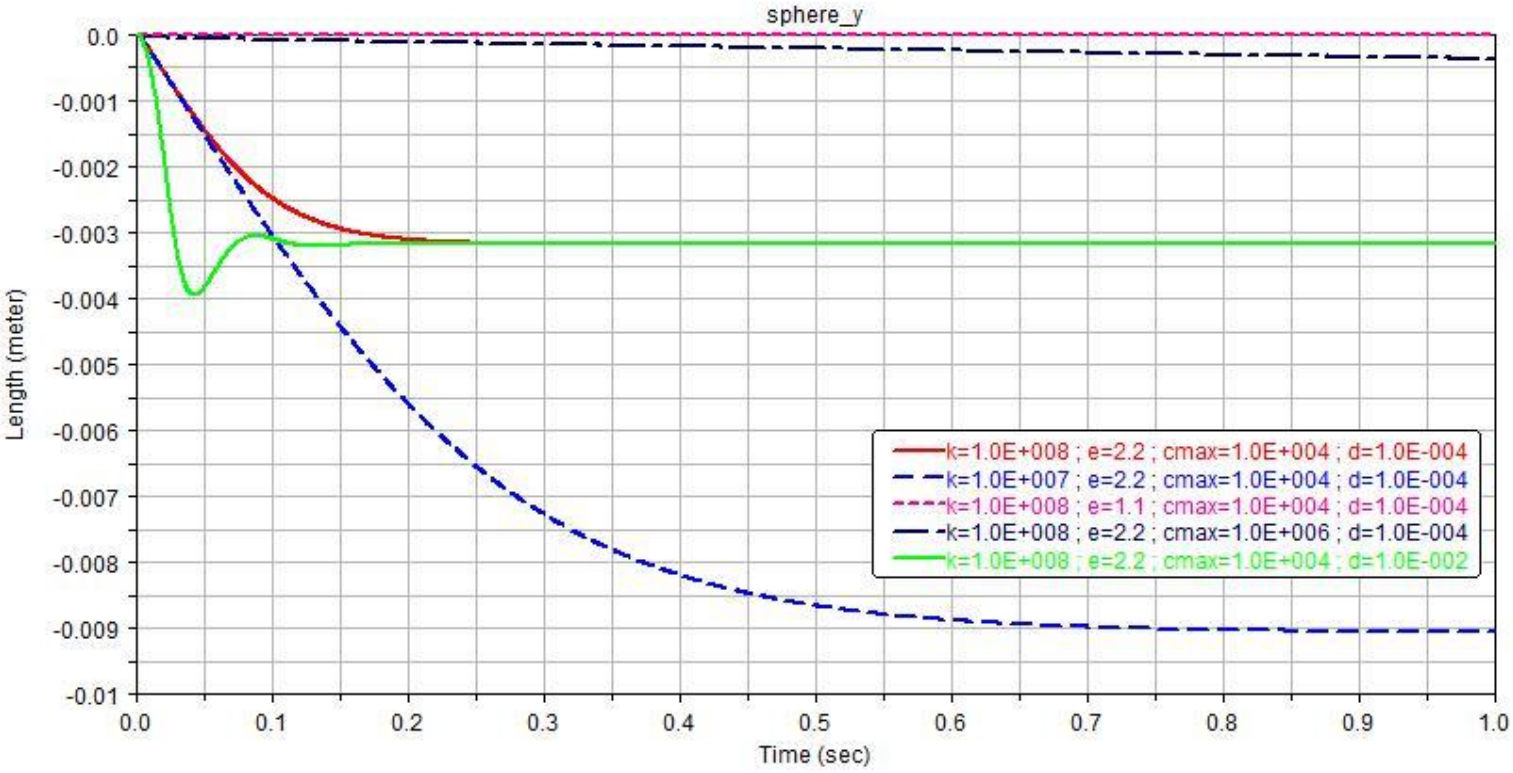

Figure 19: The Y-coordinate of the sphere for different configurations for the IMPACT function.

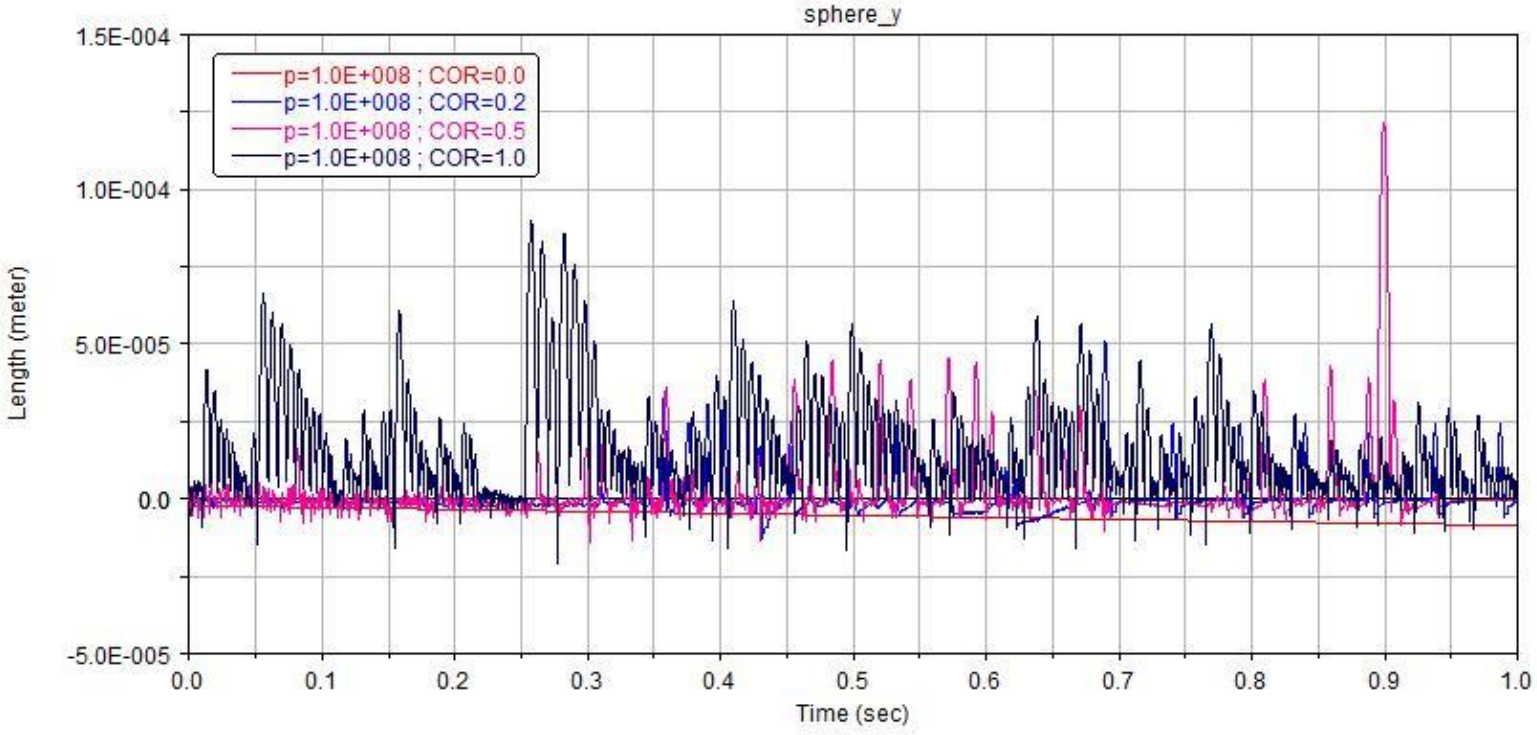

Figure 18: The Y-coordinate of the sphere for different configurations for the POISSON restitution method.

Appendix B (Rolling Ball Graphs - Continued):

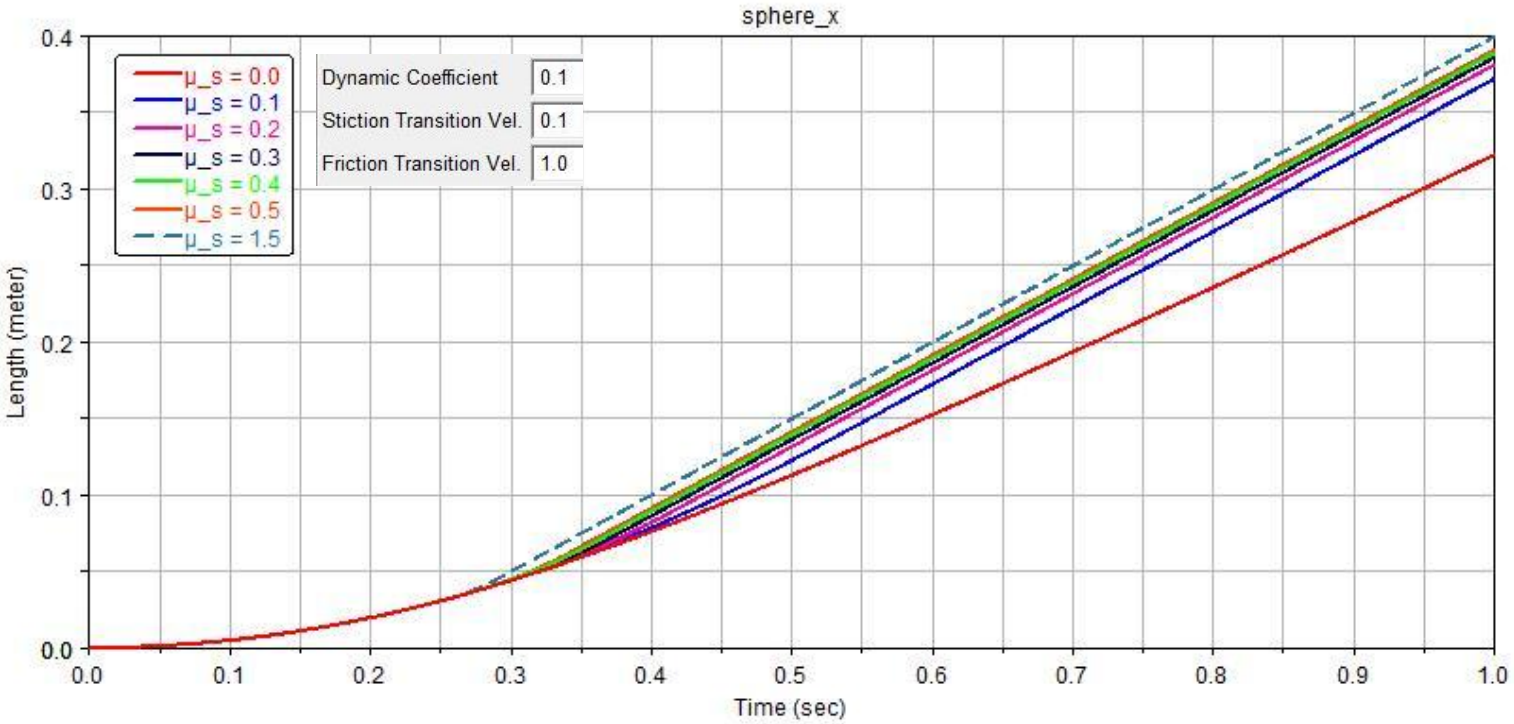

Figure 21: The X-coordinate of the sphere for different values of the static friction coefficient.

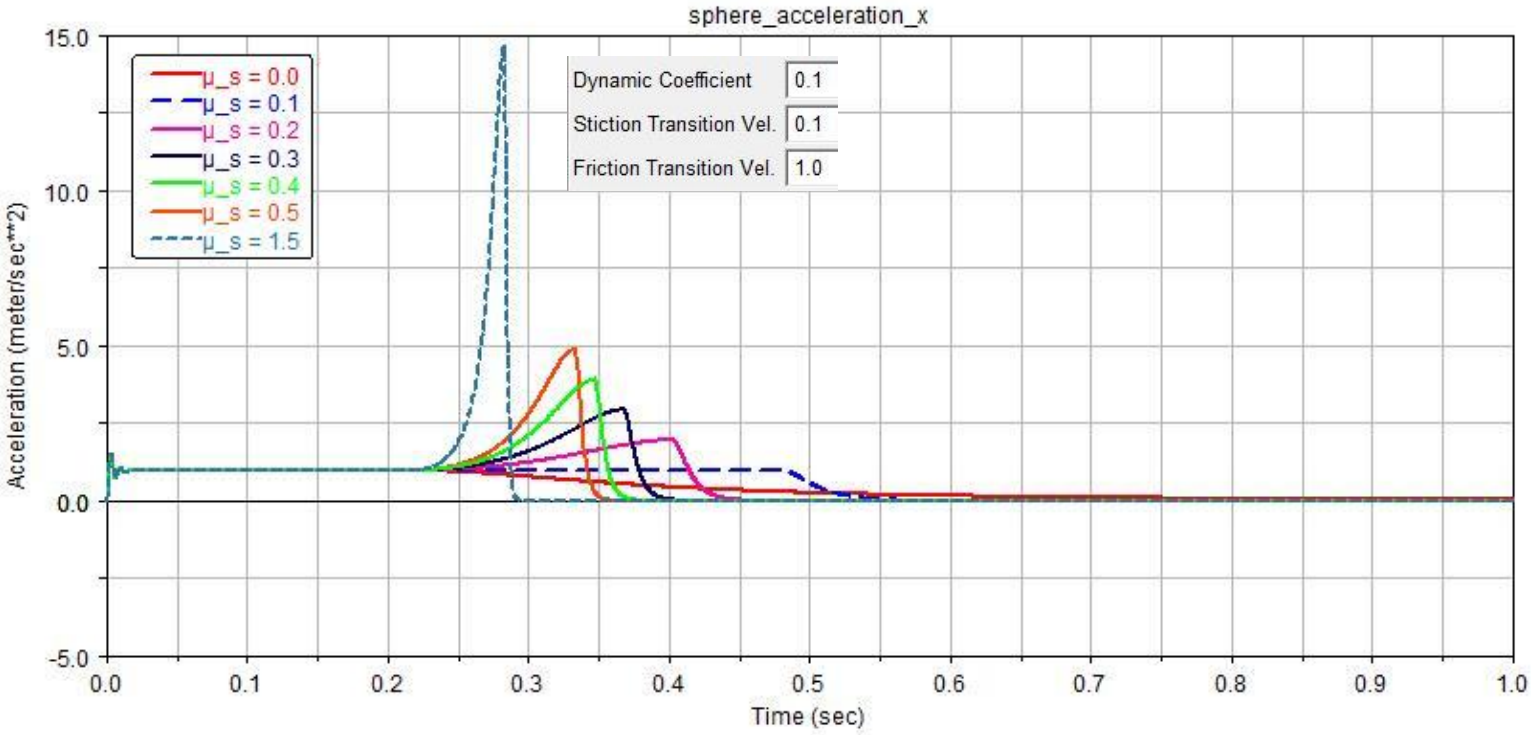

Figure 20: The acceleration in the X-direction for different values of the static friction coefficient.

Appendix B (Rolling Ball Graphs - Continued):

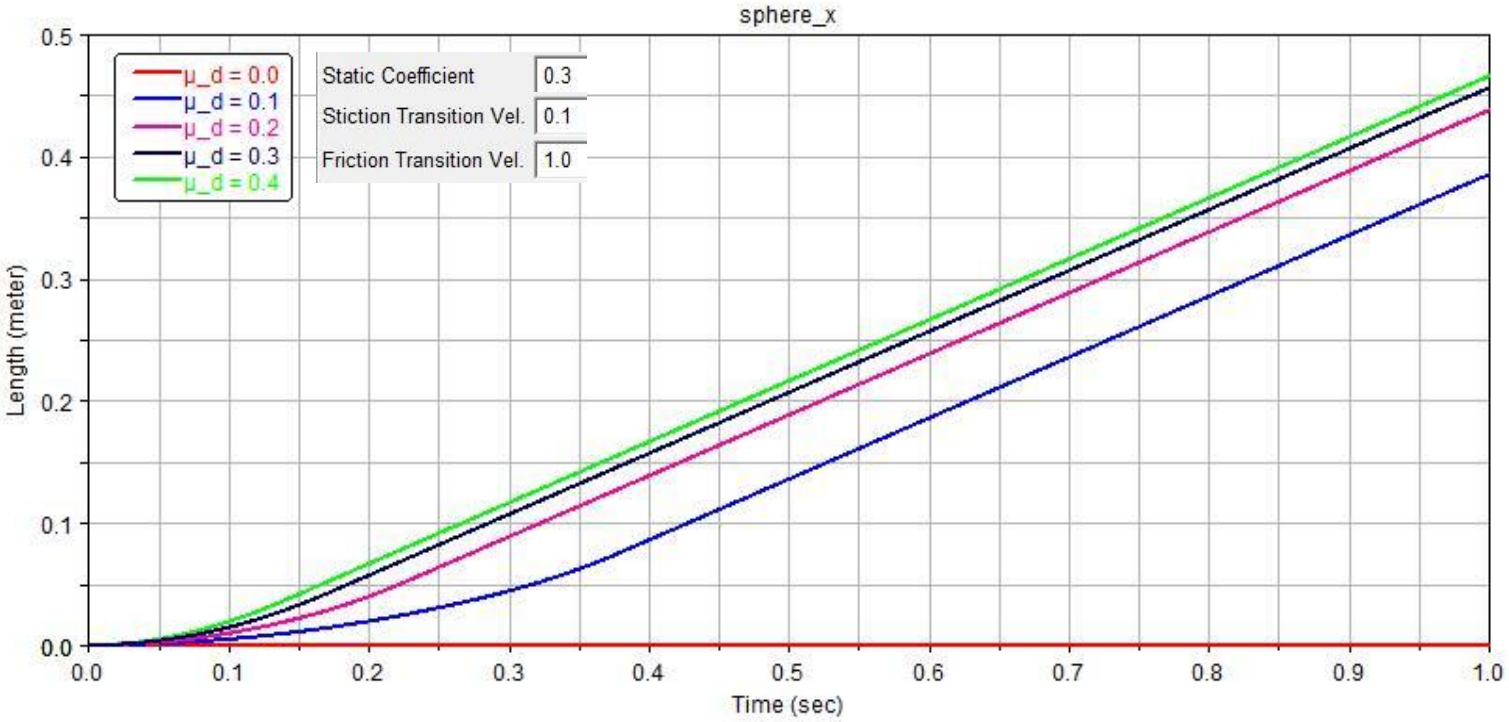

Figure 23: The X-coordinate of the sphere for different values of the dynamic friction coefficient.

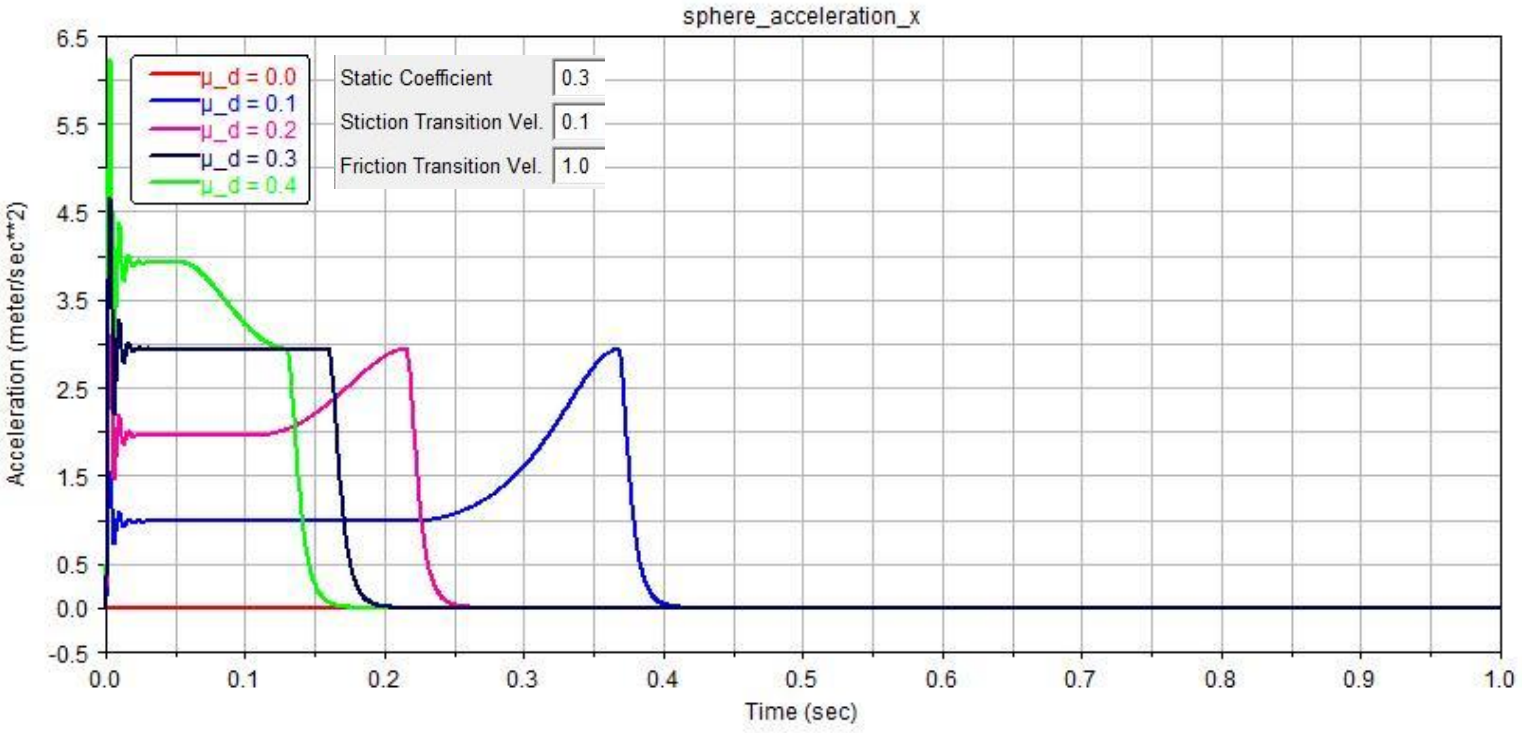

Figure 22: The acceleration in the X-direction for different values of the dynamic friction coefficient.

Appendix B (Rolling Ball Graphs - Continued):

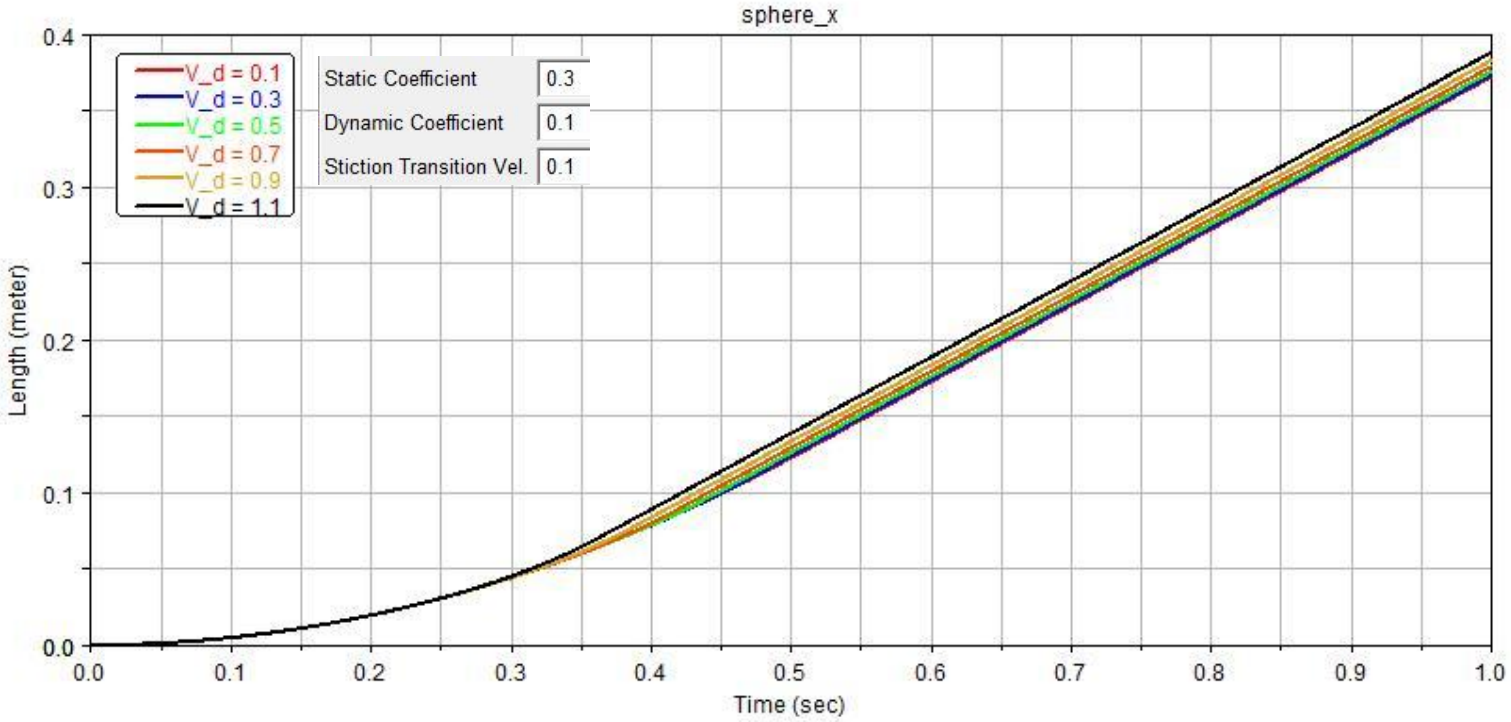

Figure 25: The X-coordinate of the sphere for different values of the friction transition velocity.

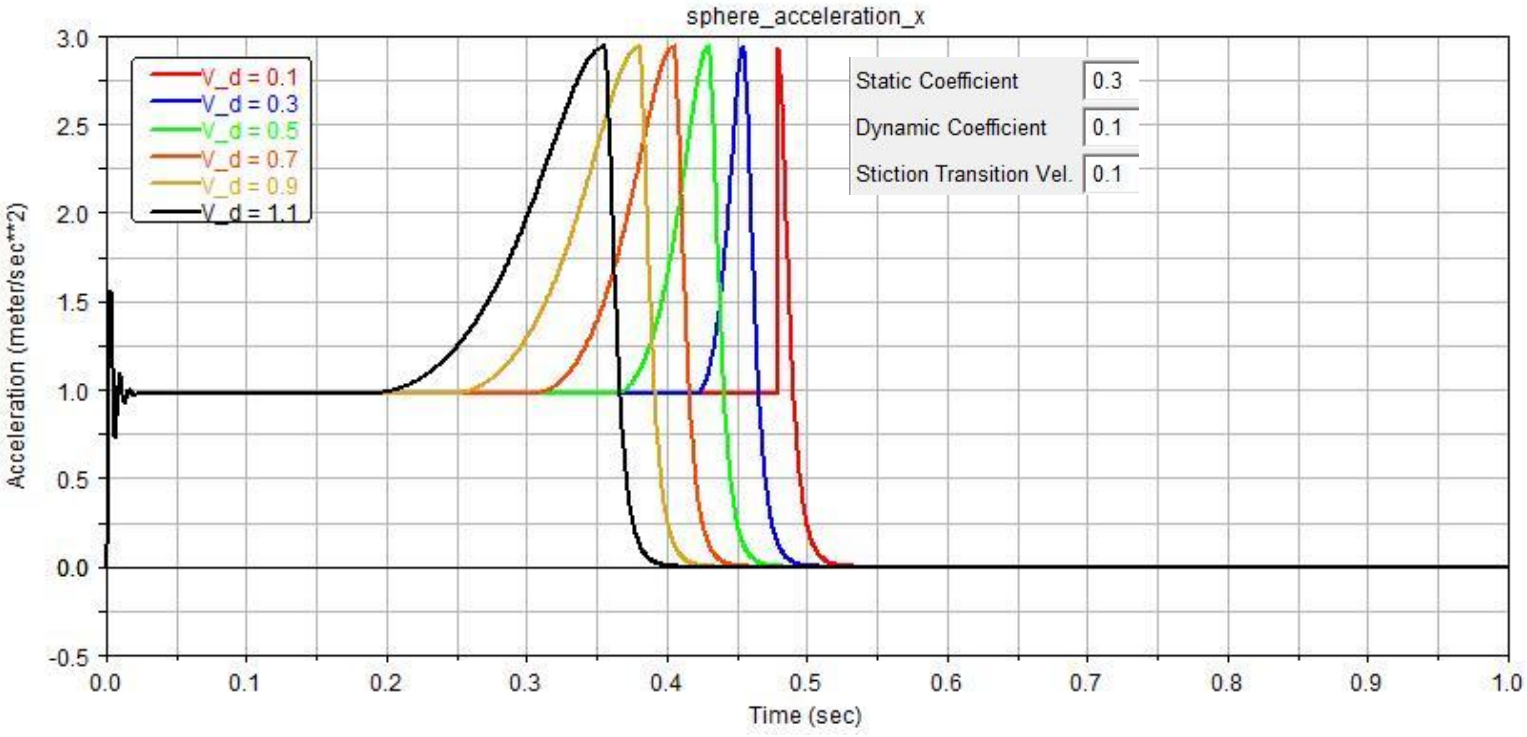

Figure 24: The acceleration in the X-direction for different values of the friction transition velocity.

Appendix B (Rolling Ball Graphs - Continued):

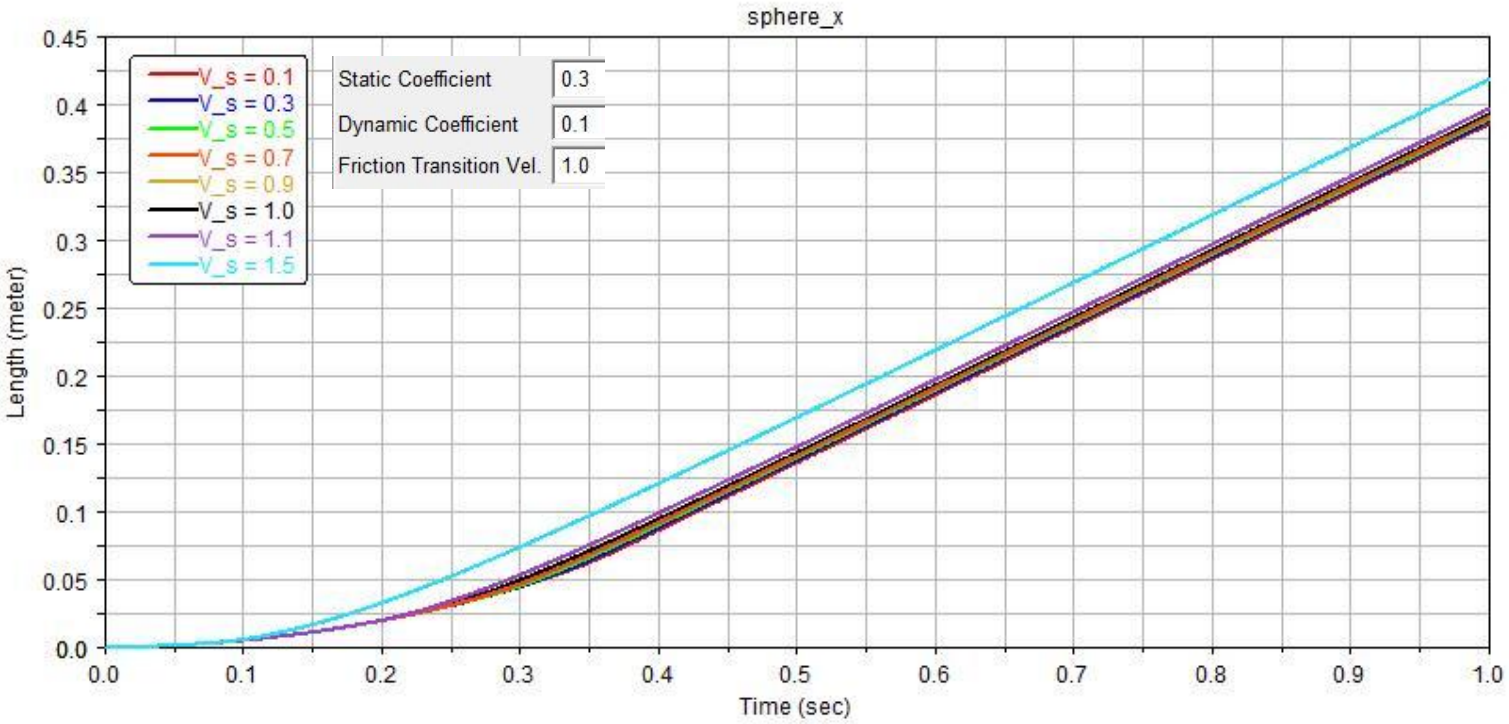

Figure 27: The X-coordinate of the sphere for different values of the stiction transition velocity.

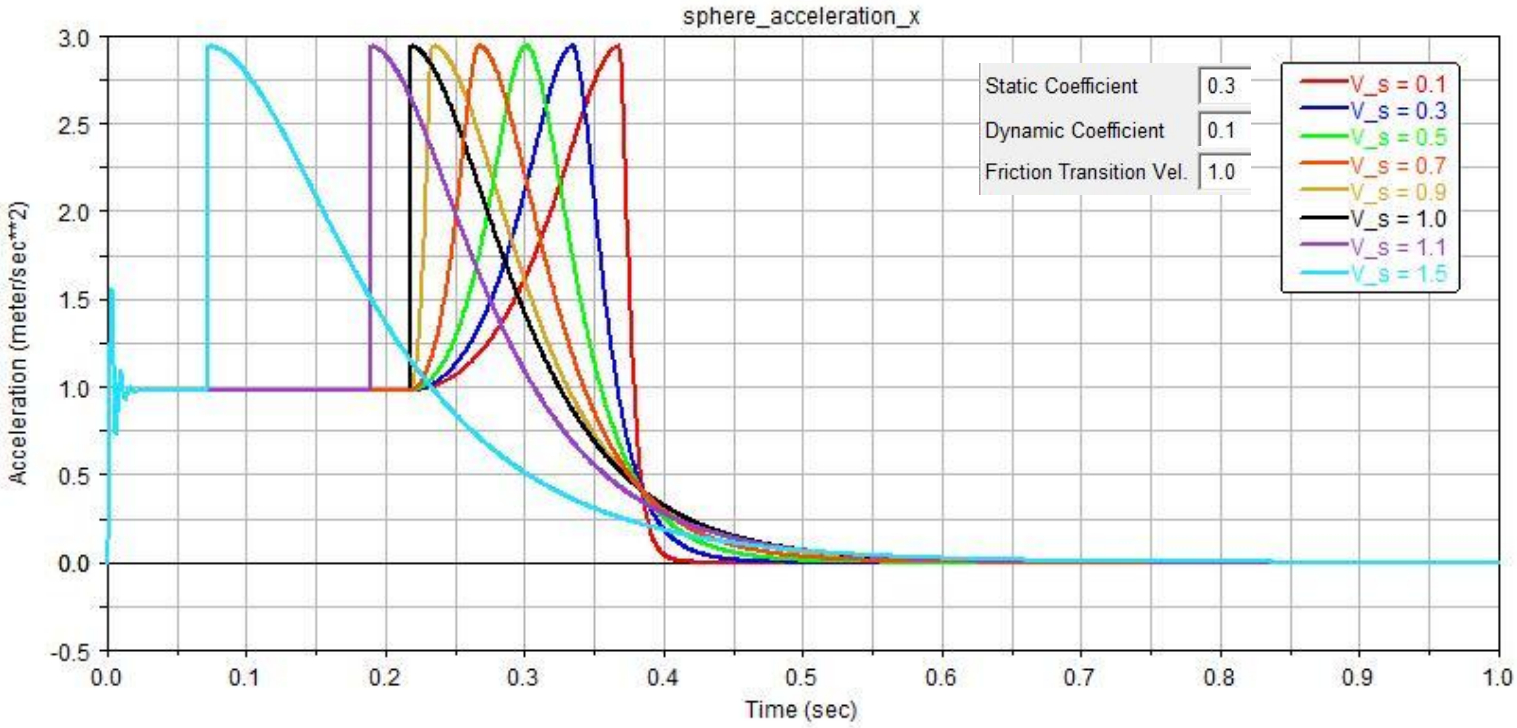

Figure 26: The acceleration in the X-direction for different values of the stiction transition velocity.

Appendix C (Material Contact Properties):

Material 1	*Material 2*	μ_s	μ_d	COR
Dry steel	Dry steel	0.70	0.57	0.80
Greasy steel	Dry steel	0.23	0.16	0.90
Greasy steel	Greasy steel	0.23	0.16	0.90
Dry aluminium	Dry steel	0.70	0.50	0.85
Dry aluminium	Greasy steel	0.23	0.16	0.85
Dry aluminium	Dry aluminium	0.70	0.50	0.85
Greasy aluminium	Dry steel	0.30	0.20	0.85
Greasy aluminium	Greasy steel	0.23	0.16	0.85
Greasy aluminium	Dry aluminium	0.30	0.20	0.85
Greasy aluminium	Greasy aluminium	0.30	0.20	0.85
Acrylic	Dry steel	0.20	0.15	0.70
Acrylic	Greasy steel	0.20	0.15	0.70
Acrylic	Dry aluminium	0.20	0.15	0.70
Acrylic	Greasy aluminium	0.20	0.15	0.70
Acrylic	Acrylic	0.20	0.15	0.70
Nylon	Dry aluminium	0.10	0.06	0.70
Nylon	Greasy aluminium	0.10	0.06	0.70
Nylon	Acrylic	0.10	0.06	0.65
Nylon	Nylon	0.10	0.06	0.70
Dry rubber	Dry steel	0.80	0.76	0.95
Dry rubber	Greasy steel	0.80	0.76	0.95
Dry rubber	Dry aluminium	0.80	0.76	0.95
Dry rubber	Greasy aluminium	0.80	0.76	0.95
Dry rubber	Acrylic	0.80	0.76	0.95
Dry rubber	Nylon	0.80	0.76	0.95
Dry rubber	Dry rubber	0.80	0.76	0.95
Greasy rubber	Dry steel	0.63	0.56	0.95
Greasy rubber	Greasy steel	0.63	0.56	0.95
Greasy rubber	Dry aluminium	0.63	0.56	0.95
Greasy rubber	Greasy aluminium	0.63	0.56	0.95
Greasy rubber	Acrylic	0.63	0.56	0.95
Greasy rubber	Nylon	0.63	0.56	0.95
Greasy rubber	Dry rubber	0.63	0.56	0.95
Greasy rubber	Greasy rubber	0.63	0.56	0.95

Table 1[15]: Material contact properties; μ_s, μ_d and COR for X combinations of materials.

[15] MSC Software, Adams/Solver help, p42/43; http://simcompanion.mscsoftware.com/infocenter/index?page=content&id=DOC9391